DEPARTMENT OF THE NAVY
NAVAL SHIP RESEARCH AND DEVELOPMENT CENTER
WASHINGTON, D.C. 20007

CAVITATION AND OPEN-WATER PERFORMANCE TESTS OF A SERIES OF PROPELLERS DESIGNED BY LIFTING-SURFACE METHODS

by

Stephen B. Denny

September 1968

Report 2878

TABLE OF CONTENTS

LIST OF FIGURES

LIST OF TABLES

NOTATION

A_E	Expanded blade area
A_o	Disk area πR^2
A_E/A_o	Expanded area ratio
B.T.F.	Blade thickness fraction
C_D	Section drag coefficient
C_L	Section lift coefficient
C_o	Section camber
C_T	Thrust coefficient $C_T = \dfrac{T}{\rho/2\ A_c\ V_A^2}$
c	Section chord length
D	Propeller diameter
g	Acceleration due to gravity
H	Hydrostatic head at shaft centerline minus vapor pressure
IVTV	Inception of visual tip vortices
J	Advance coefficient
K	Camber correction coefficient
K_Q	Torque coefficient $K_Q = \dfrac{Q}{\rho n^2 D^5}$
K_T	Thrust coefficient $K_T = \dfrac{T}{\rho n^2 D^4}$
M.W.R.	Mean width ratio
n	Propeller revolutions per second
P	Propeller section pitch
Q	Propeller torque
R	Propeller radius
r	Radial distance from propeller axis

R_n	Reynolds number at 0.7R; $R_n = \frac{c_{0.7}\sqrt{V_A^2 + (0.7\pi nD)^2}}{\nu}$
T	Propeller thrust
t	Maximum thickness of propeller blade section
V_A	Speed of advance of propeller
x	Nondimensional radius; x = r/R
Z	Number of blades
α_i	Angle of attack, two-dimensional viscous correction for NACA a = 1.0 mean line
α_t	Pitch correction due to thickness
η_o	Propeller open-water efficiency; $\eta_o = \frac{TV_A}{2\pi nQ}$
ν	Kinematic viscosity of water
ρ	Density of water
σ	Cavitation number based on vapor pressure; $\sigma = \frac{2gH}{V_A^2}$

ABSTRACT

Results of cavitation inception and performance tests are presented for a series of model propellers designed using lifting-surface procedures. Open-water performance curves are shown in addition to cavitation inception and cavitation performance data obtained in the NSRDC 24-inch variable-pressure water tunnel. The propeller series included geometrical variations of blade area, thickness, skew, and section mean-lines. Photographs are presented to compare cavitation on propellers with different blade areas and skew and operating at identical cavitation numbers and advance coefficients.

In open water, the propellers operated near their design performance, indicating that the procedure used for calculating the lifting-surface corrections is satisfactory. For very large blade areas, however, the lifting-surface pitch corrections tended to be high; for extremely thick blade sections, the pitch corrections due to thickness were too small to sufficiently account for the altered flow resulting from thick sections. For propellers with constant chordwise loading (a = 1.0 meanline), no suitable modification to two-dimensional sections was found to correct for the increased viscous effects in three-dimensional flow.

ADMINISTRATIVE INFORMATION

This work was carried out under the General Hydromechanics Research Program of the Naval Ship Research and Development Center. Funding was under Subproject S-R009-0101, Problem 526-806.

INTRODUCTION

In recent years, considerable improvements have been made in marine propeller design procedures. No longer must the designer depend on pure empirical corrections of lifting-line theoretical results to approximate lifting-surface effects in the mathematical model. Methods developed by Kerwin,[1] Pien and Cheng,[2,3] Cox,[4] and others permit the lifting surface and its influence on local flow to be accounted for throughout the design procedure.

---

[1]References are listed on page 34.

One of these methods was chosen for the design of a series of three-bladed propellers for use in unsteady force experiments in the 24-in. water tunnel. This series of six propellers represented three variations in blade area, two in blade thickness, two in chordwise camber distribution, and two in skew. Each propeller was designed for optimum performance in uniform flow. The propellers, numbered 4118, 4119, 4132, 4133, 4142, and 4143, were designed using Lerbs induction factors[5] with thickness[6] and lifting-surface influences determined by the Kerwin method; Kerwin lifting-surface calculations were used in the designs since no other suitable procedures were available at the time the study was initiated.

Open-water performance tests of the propellers indicated that the designs operated near their desired performance and that the series merited a more complete evaluation. Accordingly, cavitation inception and performance tests were conducted in the NSRDC 24-in. variable-pressure water tunnel. This report presents the results of both the cavitation and open-water performance tests. Results of the cavitation tests are of use only in giving possible information on the adequacy of the lifting-surface calculations since the propellers were not designed with regard to cavitation performance.

The variation in the propellers tested and the results of the tests yielded definite information concerning the parameters of blade thickness and blade area and the validity of the Kerwin treatment of these two parameters. These results are discussed in detail in the following sections.

DESCRIPTION OF THE PROPELLERS

All propellers in the series were three-bladed with 0.2 radius hubs and TMB-modified NACA-66 thickness sections. They were designed to be optimum in uniform flow and to produce a thrust coefficient K_T near 0.15 at a design advance coefficient J of 0.833. A section drag coefficient C_D of 0.0085 was assumed.

Propeller Model 4118 had an expanded area ratio of 0.606 and incorporated NACA a = 0.8 sectional mean lines, since the resulting viscous effects for these mean lines are small. This propeller served as the parent propeller of the series, and subsequent designs were variations from its

basic geometry. The radial distributions of section length and thickness ratio for Propeller 4118 are given in Table 1. A drawing of the propeller is shown in Figure 1.

Propeller 4119 (Figure 2) was identical to Model 4118 except it had twice the blade thickness of the parent propeller plus an additional pitch correction for thickness. Propellers 4132 and 4133 (Figures 3 and 4) had, respectively, one-half and twice the blade area of the parent propeller. To keep the stress levels equivalent, the radial distribution of maximum thickness of Propeller 4132 was $\sqrt{2}$ times that of Propeller 4118 and the thickness distribution of Propeller 4133 was $1/\sqrt{2}$ times that of the parent.

Propeller 4142 (Figure 5) differed from 4118 in that it had NACA a = 1.0 sectional mean lines plus an angle of attack α_1, determined by:

$$\alpha_1 = 2.35\ (C_L) \cdot K$$

where $2.35(C_L)$ is the two-dimensional angle of attack[7] which for the a = 1.0 mean line is due to viscous effects. K is the camber correction coefficient, i.e., the ratio of three-dimensional camber to two-dimensional camber calculated in the Kerwin method; it was applied in the calculation of α_1 in an attempt to correct for the three-dimensional effects.

Basic differences in the propeller geometries are designated in Table 2. The radial distributions of pitch and camber are presented as nondimensional quantities in Tables 3 and 4, respectively, and the pitch corrections due to thickness for all the propellers are shown in Table 5.

Model Propeller 4143 (Figure 6), also identified in the tables, was a highly skewed propeller and was initially conceived to belong to the aforementioned series. It had the same section length and thickness distributions as the parent propeller (4118) but was skewed 15 deg for each one-tenth radius from the hub; this resulted in a total skew at the tip of 120 deg. However, a misinterpretation of skew notation in the computer program input produced lifting-surface angle of attack corrections which were quite different from those appropriate for the skewed propeller. Discovery of the designing error occured after completion of construction and testing and after check calculations were made with the Pien method[3] and Kerwin's latest design program.[10] Table 6 compares pitch distribution of the present Propeller 4143 with that derived for the correct design.

PROCEDURE AND RESULTS

Open-water testing was carried out at this Center with the propellers driven from downstream and mounted on the standard propeller boat. Propeller thrust and torque were determined over a range of advance coefficients from zero to 1.30. Water speed and propeller revolutions were sufficiently high to produce a minimum Reynolds number at the 0.7 radius of 5.0×10^5. Open-water performance curves for the six propellers are shown in Figures 7-12. Table 7 compares the experimentally determined performance of each propeller with its predicted performance. The comparisons were made using the nondimensional coefficients of thrust K_T, torque K_Q, and efficiency η_o which were determined while the propellers were operating at design $J = 0.833$.

As mentioned before, the predicted performance was based on calculations using section drag coefficients equal to 0.0085. A reanalysis of propeller designs was carried out using the best available drag data[8] which consider section thickness-chord and section camber ratios. This check indicated that except for Propeller 4133, the design thrust coefficients (Table 7) were within 0.5 percent of the later calculations. The thrust coefficient calculated for 4133 using the section drag data was 1.5 percent greater than that determined using a constant $C_D = 0.0085$. Torque coefficients calculated using the better drag data were less than those shown in Table 7. They were as follows: K_Q (4118), - 2.5 percent; K_Q (4119), - 1.8 percent; K_Q (4132), - 0.2 percent; K_Q (4133), - 5.1 percent; K_Q (4142), - 2.5 percent; K_Q (4143), - 1.3 percent. The accuracy of the open-water tests should also be mentioned. Error in the advance coefficient is negligible. Quoted values of the thrust and torque at a particular advance condition are within 2.0 percent of the true value when considering both the dynamometer accuracy and the possible error in reading the dynamometer. Fairing of the data in the open-water curves produces even greater accuracy. It should be emphasized that the use of K_T and K_Q coefficients in Table 7 is rather a severe means of comparing design and experimental performance. In the practical case, a ship operates at neither constant J nor constant K_T, but rather approximately at a constant thrust coefficient C_T which is proportional to K_T/J^2. The propellers are compared on this basis in Table 8.

Cavitation inception and performance testing was conducted in the 24-in. water tunnel with the propellers mounted on the downstream shaft and in the open-jet test section. The aluminum constructed propellers were anodized and dyed black and had each 0.1 radius marked in white to facilitate cavitation inception visualization. Thrust and torque were measured with the 150-hp dynamometer and water speeds in the tunnel tests were determined by establishing a thrust identity with the open-water test results. Throughout the cavitation inception and performance testing, water speeds were in the range of 8.0 to 15.0 ft/sec and propeller revolutions were set between 20 and 25 rps.

Inception points at each advance condition were established by setting constant water speed and propeller revolutions and then decreasing tunnel pressure until cavitation developed. Static pressure values entering into the calculation of cavitation number are those pressures at the propeller shaft line. During the runs, air content was maintained between 15 and 30 percent of saturation at atmospheric pressure.

Since a thrust identity with the open-water test results was necessary for determining tunnel water speed, a sizeable error could result in the determination of the cavitation number for an experimental condition. If a maximum error of 2.0 percent in thrust is assumed in setting a desired thrust, a similar percentage error in water speed is possible. This, entered into the calculation of the cavitation number, could produce a possible maximum error of 4.0 to 5.0 percent, considering errors in pressure measurement and rps to be negligible.

The inception curves (Figures 13 to 18) show the extent of radial cavitation from the tip as a function of advance and cavitation number. These curves show the occurrence of face (pressure side) cavitation at the higher advance conditions and back (suction side) at lower advances. The area above a curve indicates that no cavitation was present at the designated radius for the particular value of advance and cavitation number. At and below a radial inception curve, cavitation was present and the intensity increased with a decrease in σ. The entire system of curves, therefore, enables one to determine the extent of cavitation at any value of advance and cavitation number within the range presented.

Curves designated IVTV denote the inception of visual tip vortices. For all the propellers tested, cavitation of the vortices first appeared downstream and later became attached to the propeller blade tips. The eventual attachment of the vortices to the propeller was recorded as the $x = 1.0$ inception curve.

Back cavitation was mainly sheet cavitation and most frequently developed at the leading edge of the blade. Intermittent bubble cavitation occurred occasionally on the propellers at high advance ratios and very low cavitation numbers, and no attempt was made to systematically record it.

During cavitation inception tests of the Propellers 4118, 4132, 4138, and 4143 (Figure 19), thrust and torque breakdown due to cavitation was recorded. Figures 20 through 23 show the thrust and torque coefficient curves over a range of J for cavitation numbers of 10.0, 5.0 and 2.0. These values are superimposed on those thrust and torque curves of the noncavitating open-water tests of each propeller. Photographs of the four propellers are shown in Figures 24-28 during operation at several of the above-mentioned conditions.

DISCUSSION

Comparisons between design predictions and open-water test results (Tables 7 and 8) indicated that Propellers 4118, 4119, and 4132 were slightly underpitched. Propellers 4118 and 4132 produced thrust and torque values at advance coefficients near design which were within the accuracy of the design calculations, the experiments, and the manufacturing tolerances. However, open-water test results for the double-thickness propeller (4119) showed a discrepancy greater than could be attributed to these possible inaccuracies. Since the only geometric differences between Models 4118 and 4119 are the section thicknesses and the section pitch corrections due to thickness, it can be assumed that these theoretical corrections[6] are not sufficiently large to completely account for the altered inflow when thick sections exist. For the thicker sections, this might be expected since the calculations are based on linearized theory.

At the design advance coefficient, Propeller 4133 developed higher thrust (4.5 percent) and torque (3.8 percent) than that aimed for in its design, although rpm at the design C_T was 1.0 percent lower than the design value. Calculations made with the more accurate section drag data indicated that the thrust K_T should be 1.5 percent greater at the design condition; however, the same calculations predicted the torque coefficient to be 5.1 percent less. These results indicate that the theoretical lifting-surface corrections[4] may be too large for very wide blades, particularly in view of the generally opposite trend of the included thickness correction.

Propeller 4142 with NACA a = 1.0 sectional mean lines, was approximately 10.4 percent low in thrust and 9.0 percent low in torque at design J. At the design C_T, the rpm was 2.6 percent high. The results clearly indicate that the attempt to determine a viscous correction for the a = 1.0 mean line was not successful.

In the inception curves (Figures 13 and 14), back and face cavitation on Propeller 4119 occurs over a majority of the blade radii at lower σ values than on Propeller 4118 for corresponding high or low advance conditions. This is attributed to the presence of the wider minimum pressure envelopes[9] for the thicker sections of Propeller 4119 for significant positive or negative angles of attack.

Cavitation inception data showed small differences in radial inception versus cavitation number among Propellers 4118, 4132, and 4133. At design advance or below, the wide-bladed 4133 generated tip vortices at slightly lower σ values than the parent propeller (4118) and those generated by the narrow-bladed 4132 appeared at higher σ values than for the parent. For radii near the hub, back cavitation appeared on Propeller 4132 at lower cavitation numbers than for the other two propellers. Because it was slightly overpitched, face cavitation on Propeller 4133 occurred at lower σ values than for the parent propeller.

As a result of being underpitched, Propeller 4142 exhibited less back cavitation and more face cavitation than did the parent for identical advance coefficients and cavitation numbers. Tests of the highly skewed propeller (4143) gave the most favorable inception curves of all the propellers. For all types of cavitation, the inception curves varied less with speed coefficient than for the other propellers. The IVTV curve for this propeller was higher at the design speed coefficient but this was probably because of the inadvertently high loading near the blade tip.

Thrust and torque measurements taken during the tunnel testing for Propellers 4118, 4132, 4133, and 4143 (Figures 20-23) showed varying degrees of fall-off because of cavitation at cavitation numbers of 2.0, 5.0, and 10.0. As expected, because of blade area, Propeller 4133 suffered the least percentage fall-off in both thrust and torque for all the values of σ; Propeller 4132 suffered the greatest. The highly skewed Propeller 4143 had percentage fall-off at all σ values comparable to, if not somewhat less than, the parent 4118.

With the exception of Propeller 4143, the cavitation on the propellers showed no unusual trends. The lifting-surface corrections are not ideal for thick sections and for very large blade areas, but from the results of the cavitation tests, the radial distributions of the corrections appear good.

All of the propeller designs were recalculated using both the new Kerwin[10] propeller design program and the Cheng program described in References 3. Some differences were noted, but they should not significantly affect these comparisons.

In the performance analysis of the highly skewed propeller (4143), several points should be made. First, although a considerable error was made in designating the final design pitch, the thrust and torque coefficients from the open-water tests were only 9 to 15 percent, respectively, away from design at $J = 0.833$. This was a 2-percent error in rpm at design C_T. Before the availability of lifting-surface design procedures, even that degree of accuracy would not have been expected when designing for extensive skew. A properly derived pitch distribution should yield a further improvement in performance.

Secondly, from the cavitation inception curves of Figures 13 and 18, it can be seen that except for the inception of tip vortices, Propeller 4143 yielded better back cavitation characteristics at all radii and advance coefficients than the nonskewed parent propeller. In addition, the inception characteristics would probably have been improved even more had the appropriate pitch distribution been used since this would have meant a considerable reduction in pitch of the blade near the tip.

An understanding of the cavitation characteristics of the highly skewed propeller comes from plentiful data related to flow characteristics on swept wings. First, examine the pressure distribution on a wing or blade of considerable sweep or skew and at very low angles of attack. It is commonly accepted that the pressure distribution on such a surface is influenced by the extent of sweep or skew. Briefly, for wings of uniform cross section,[11] the minimum pressure is a direct function of the component of inflow velocity normal to the leading edge. This is not purely calculable, however, since although the sweep angle is known, the thickness chord ratio of the section acted upon by the velocity component is altered,[12] which further affects the minimum pressure. In addition, the flow on the two-dimensional wing is truly three-dimensional and the degree of deflection in the streamlines over the foil is a complicated function of the extent of sweep.

An even more complex flow phenomenon arises for swept wings or blades at high angles of attack. Here, flow separation enters into the factors influencing lift and the resulting induced pressures and velocities.

For finite angles of attack, separation occurs quite readily at the leading edge of swept wings and, in conjunction with the sweep, the separation initiates the formation of a vortex sheet. This vortex sheet curls over the wing, may or may not reattach on the wing, and may or may not begin to dissipate at the wing surface. Reattachment of the vortex sheet to the wing can considerably increase lift[13] whereas dissipation of the vortex sheet can produce large drag forces. In any instance, the vortex sheet forms readily in the presence of sweep and can definitely produce abnormal radial flow on the blades in the case of a marine propeller.

CONCLUSIONS

Performance tests reported here indicate that the lifting-surface propeller design procedure developed by Kerwin is satisfactory. As mentioned before, the propellers of the series were developed for use in fluctuating force measurements and do not necessarily represent the normal geometries expected in a marine propeller design. For instance, one would not expect to incorporate into a specific propeller design the large section thickness characteristics of Propeller 4119 or the extreme blade areas of Propellers 4132 and 4133.

The following conclusions can be made from experimental investigations:

1. The test results of Propeller 4118 and its double-thickness counterpart 4119 indicate that the incidence correction to pitch because of thickness as determined in the Kerwin procedure is not large enough to account for the altered sectional inflow resulting from thick blades. However, for the design C_T, the rpm was only 1.0 percent high for the thicker propeller.
2. Propeller 4133 was overpitched but at design C_T, it operated only 1.0 percent below the design rpm. It can be assumed that high pitch resulting from the design procedure is due to the large blade area of the propeller.
3. Propeller 4142, with NACA a = 1.0 sectional mean lines, was considerably underpitched. The necessary modifications of the two-dimensional sections to correct for the increased viscous effects in three-dimensional flow are not predictable.

4. Despite a design error, Propeller 4143 displayed reduced cavitation at low advance coefficients, when compared to parent Propeller 4118. Should correctly designed highly skewed propellers achieve predicted performance, then the reduced cavitation at low advance conditions makes the application of high skewed propellers a worthwhile area to explore. These factors, together with the advantages of reduced thrust and torque fluctuations in wake operation.[14] warrant more intensive investigation into the phenomena involving skewed propellers.

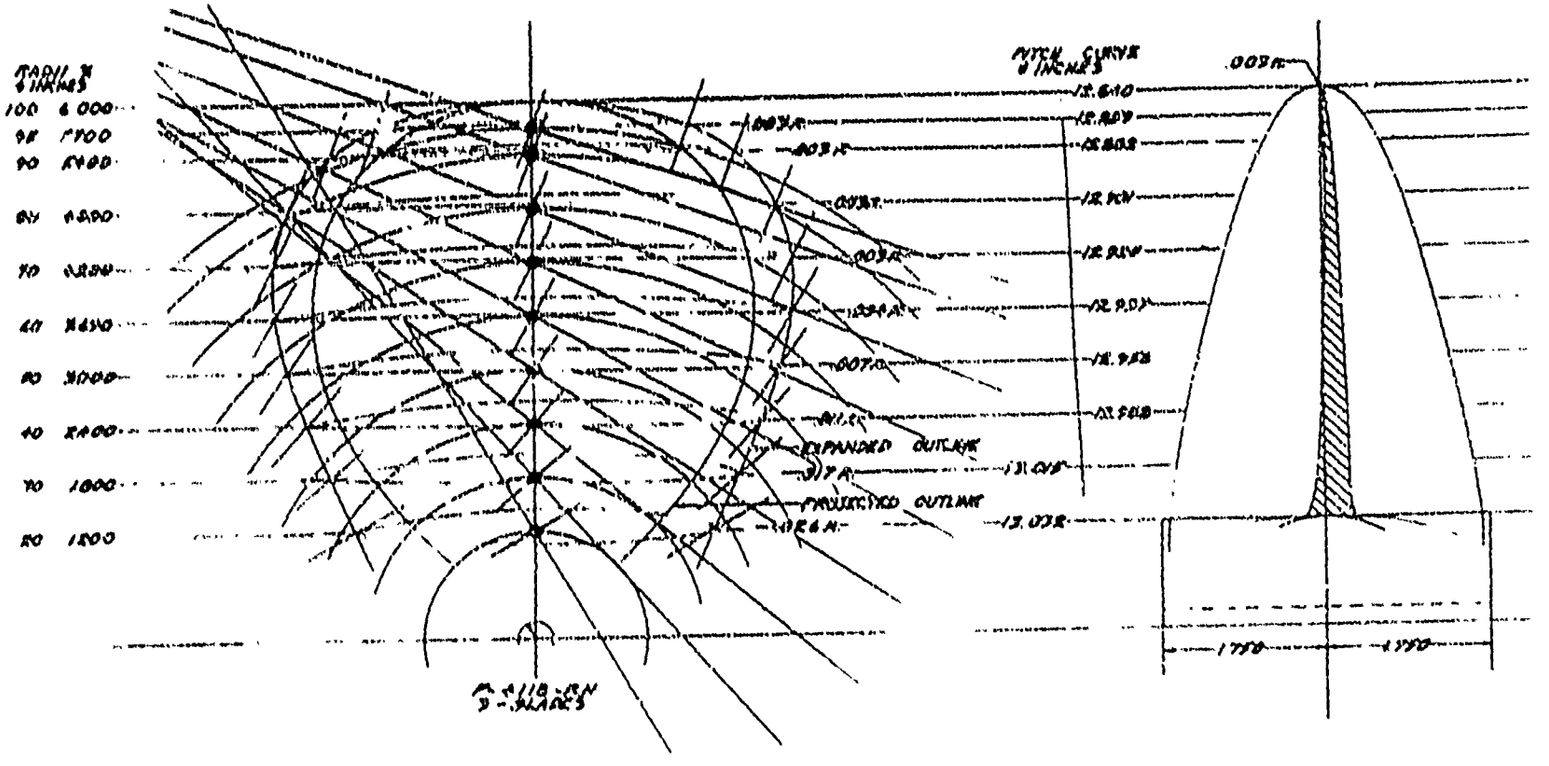

Figure 1 - Details of Propellor 4118

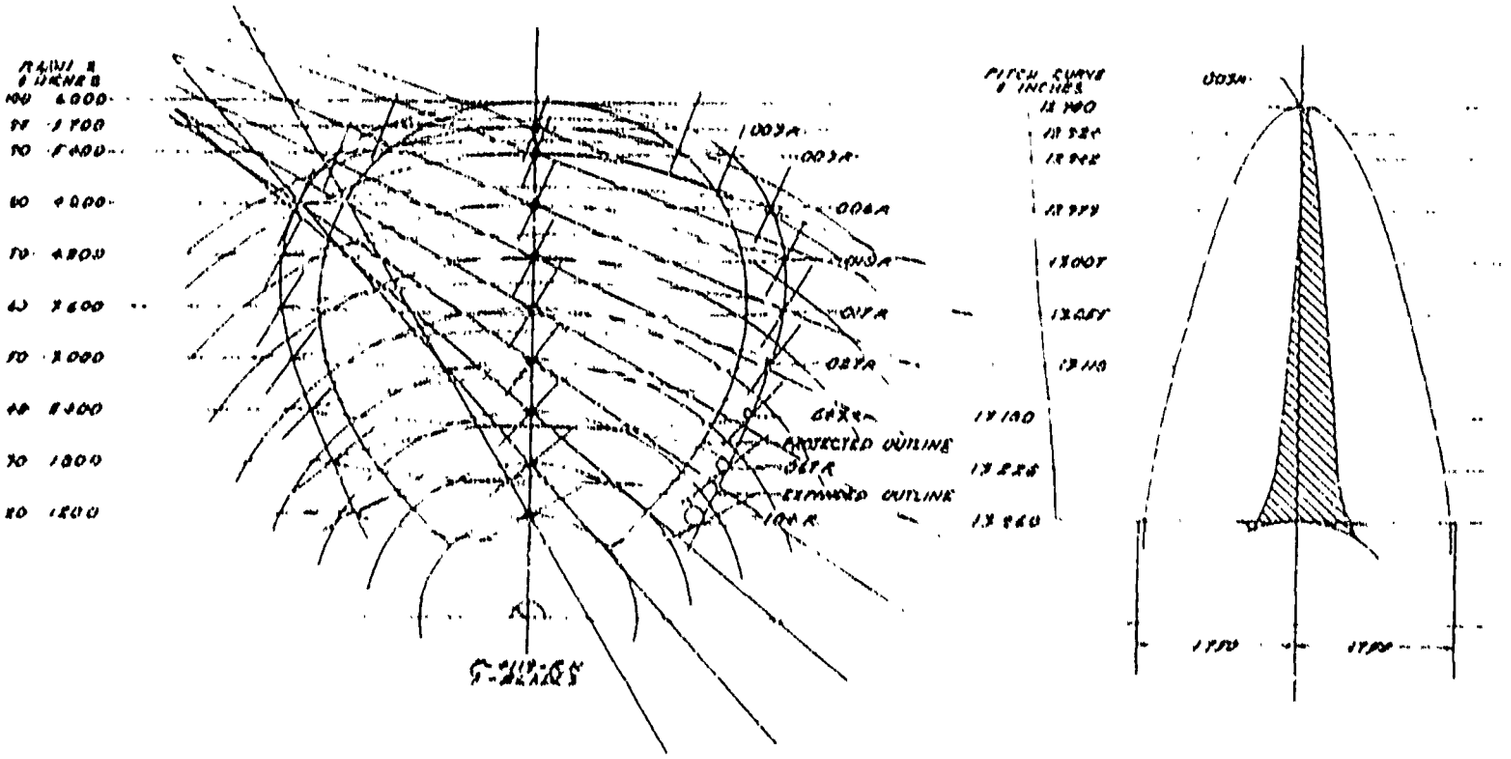

Figure 2 - Details of Propeller 4119

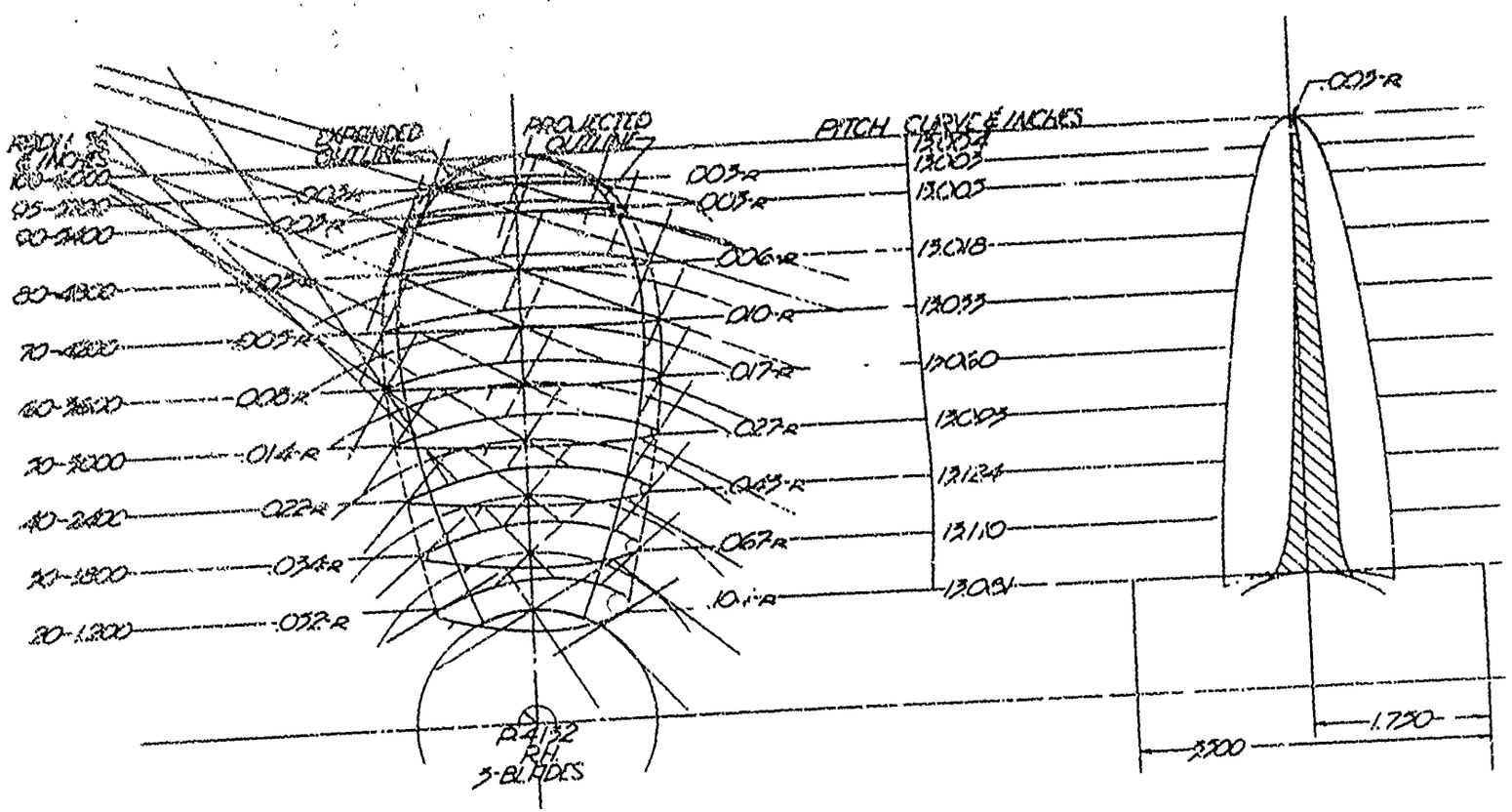

Figure 3 - Details of Propeller 4132

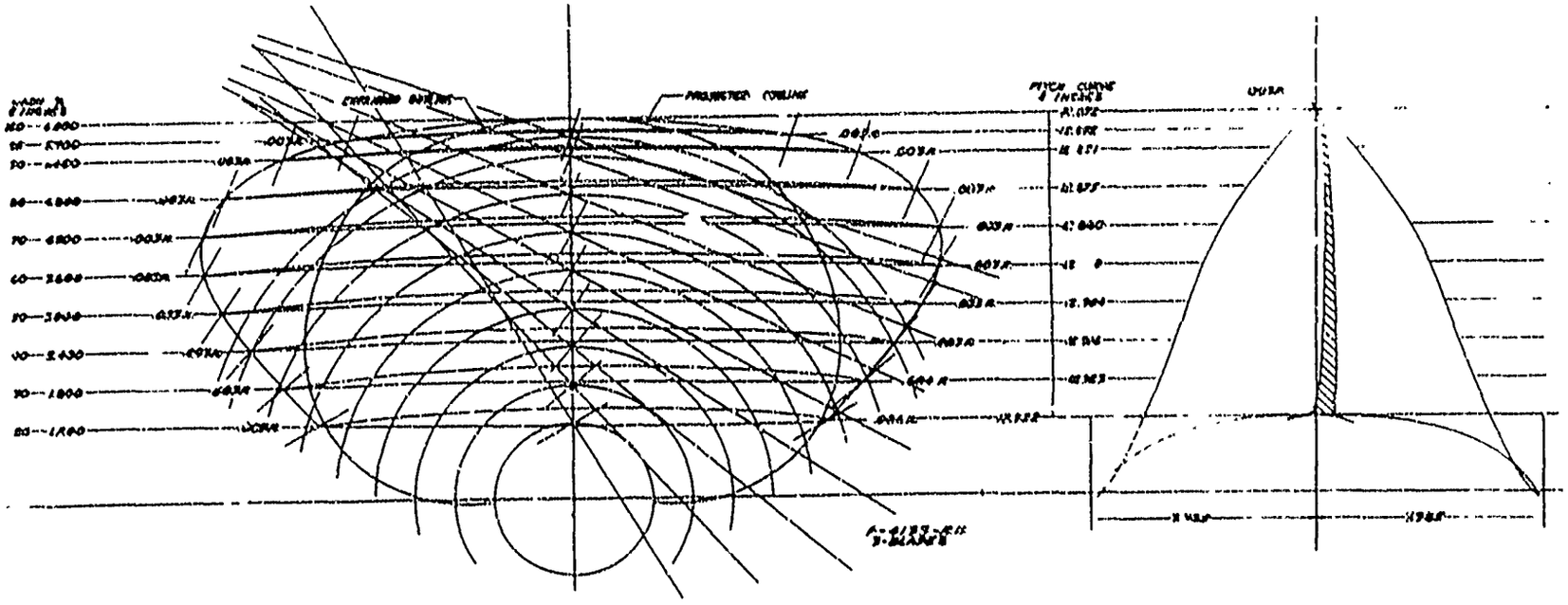

Figure 4 - Details of Propeller 4133

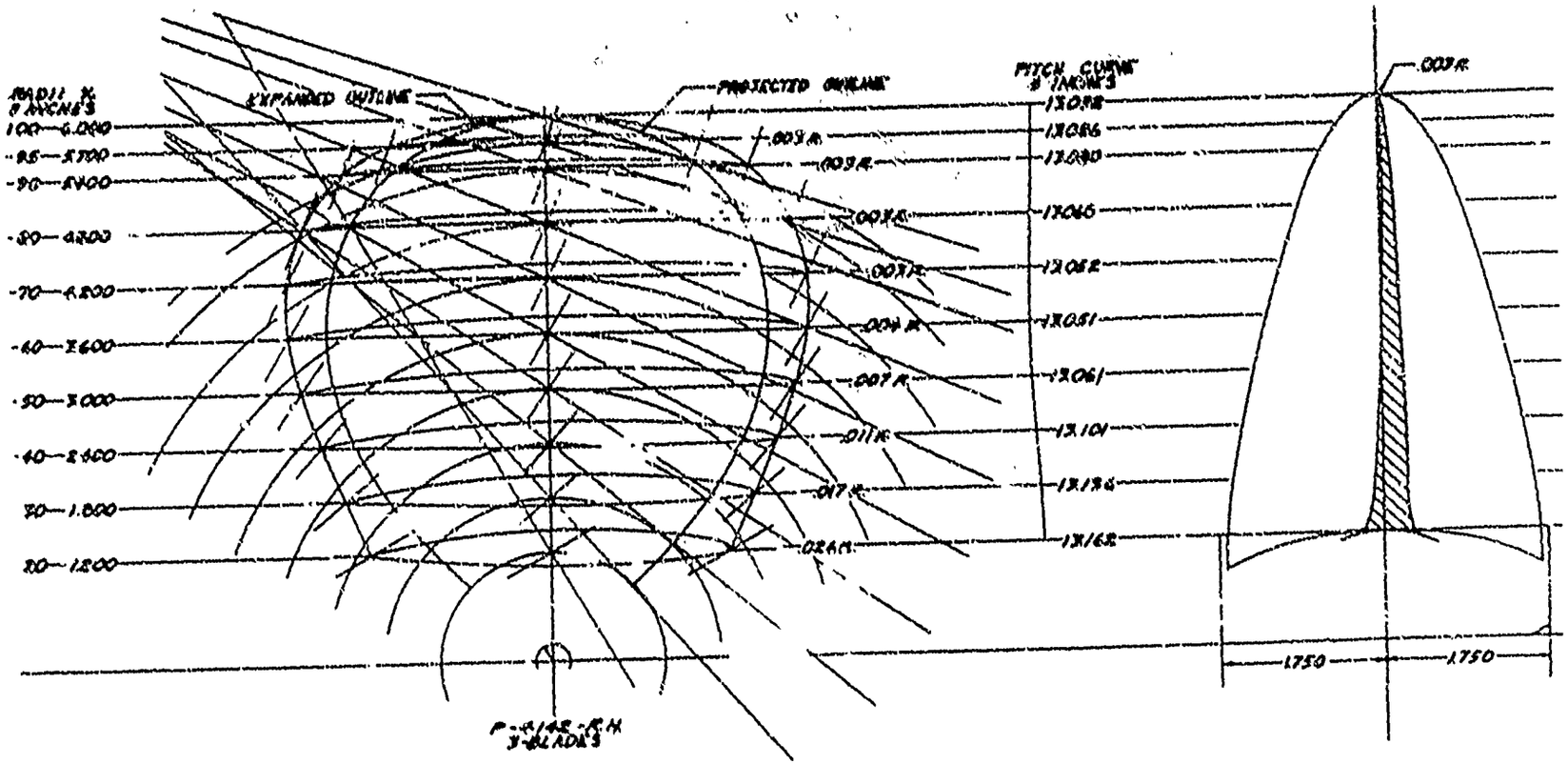

Figure 5 - Details of Propellor 4142

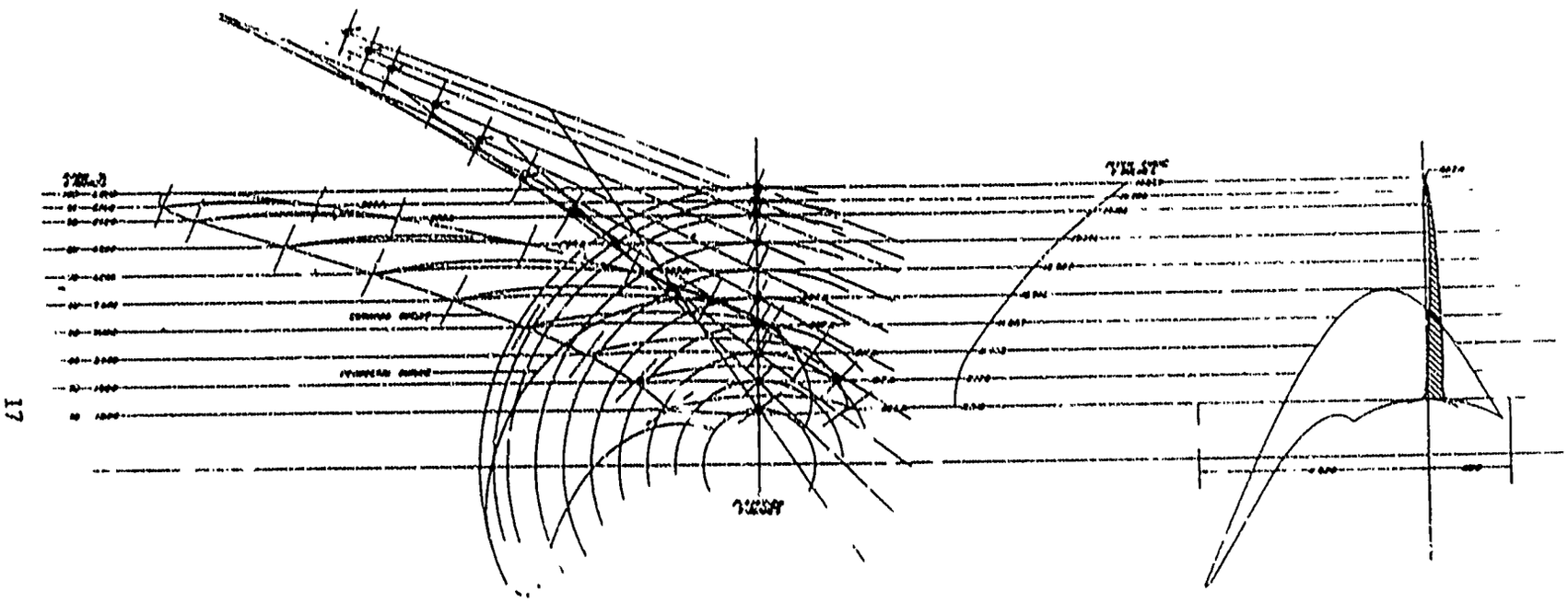

Figure 6 - Details of Propeller 4143

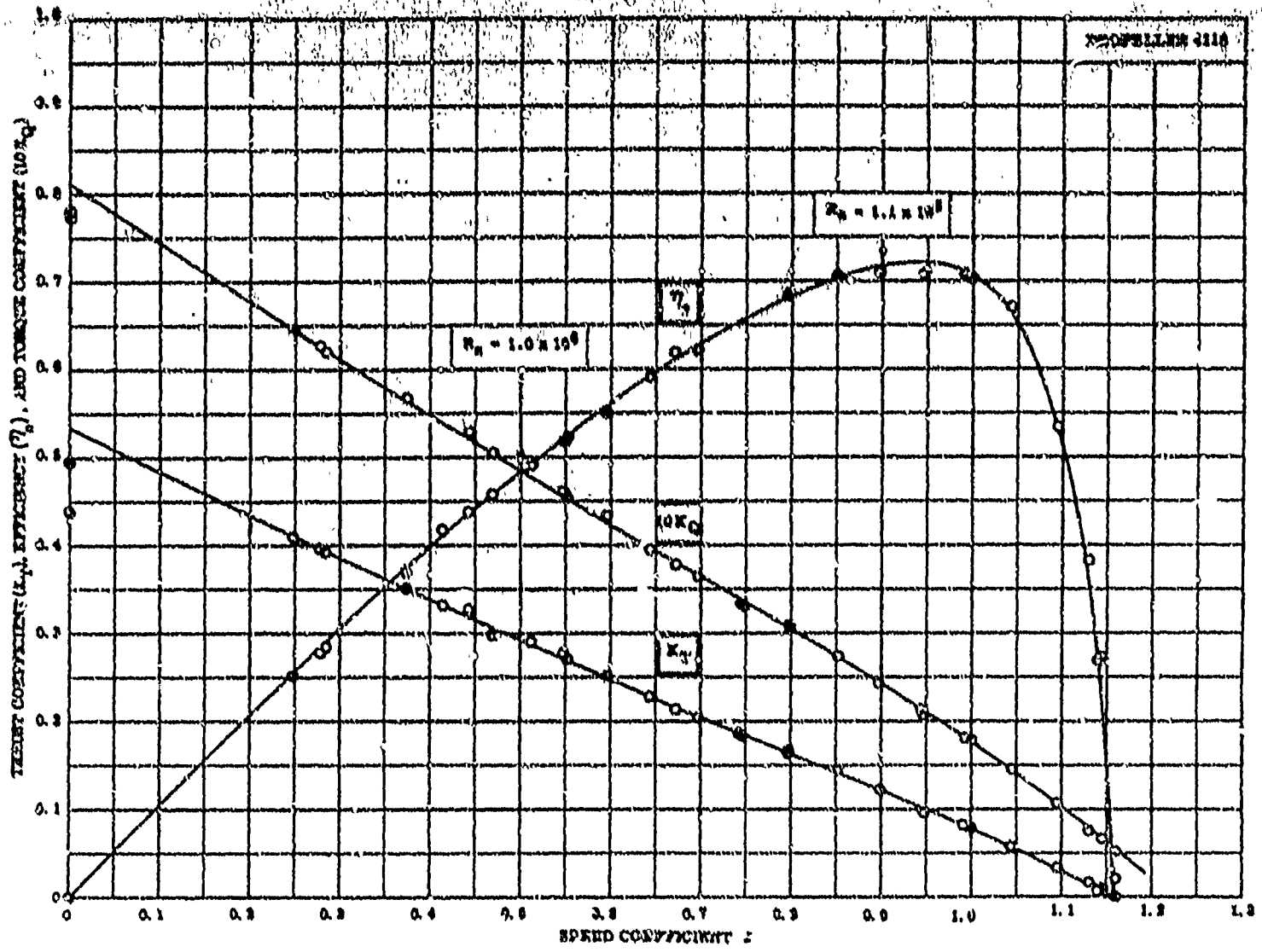

Figure 7 - Open-Water Performance Curves, Propeller 4118

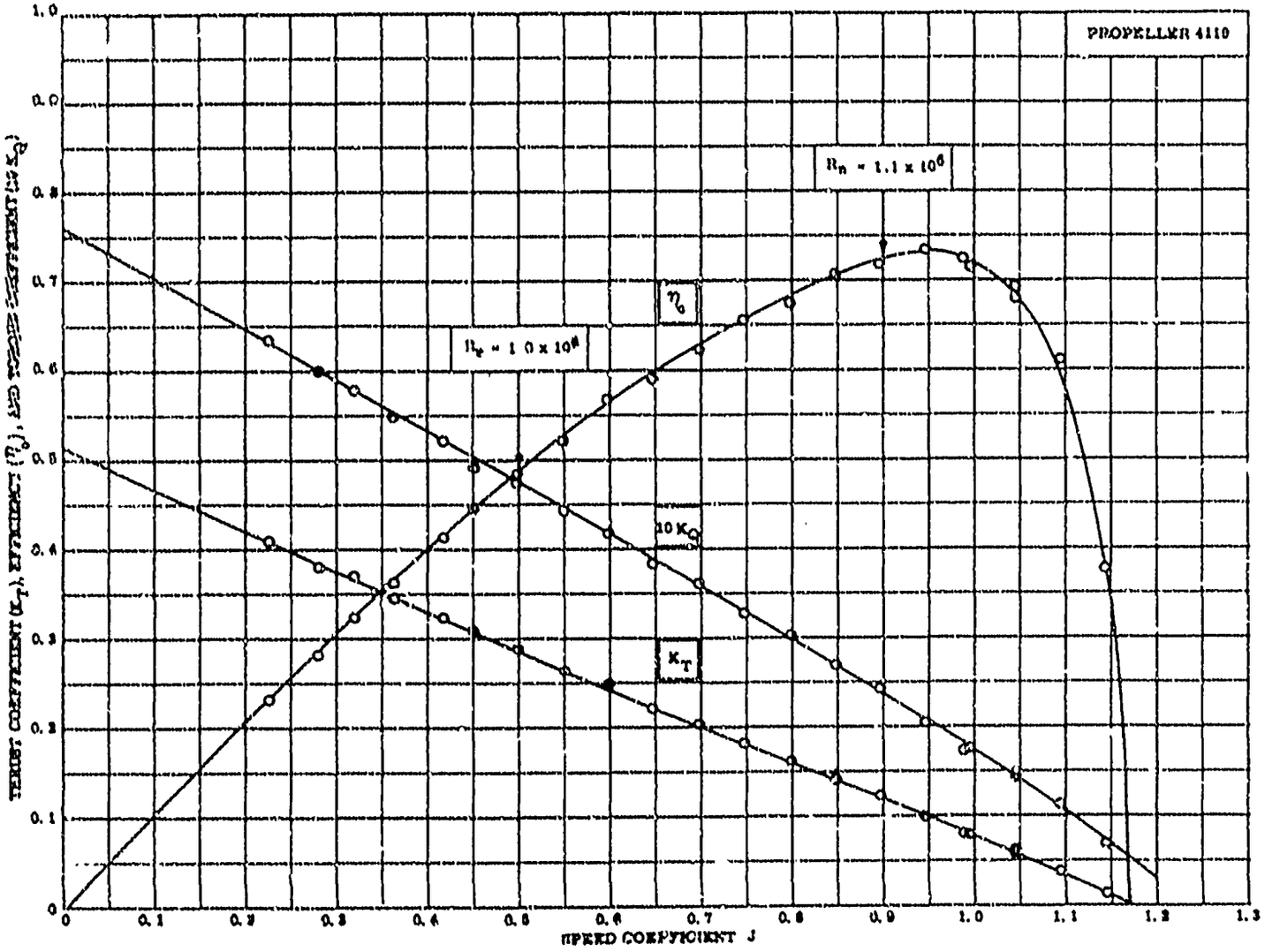

Figure 8 - Open-Water Performance Curves, Propeller 4119

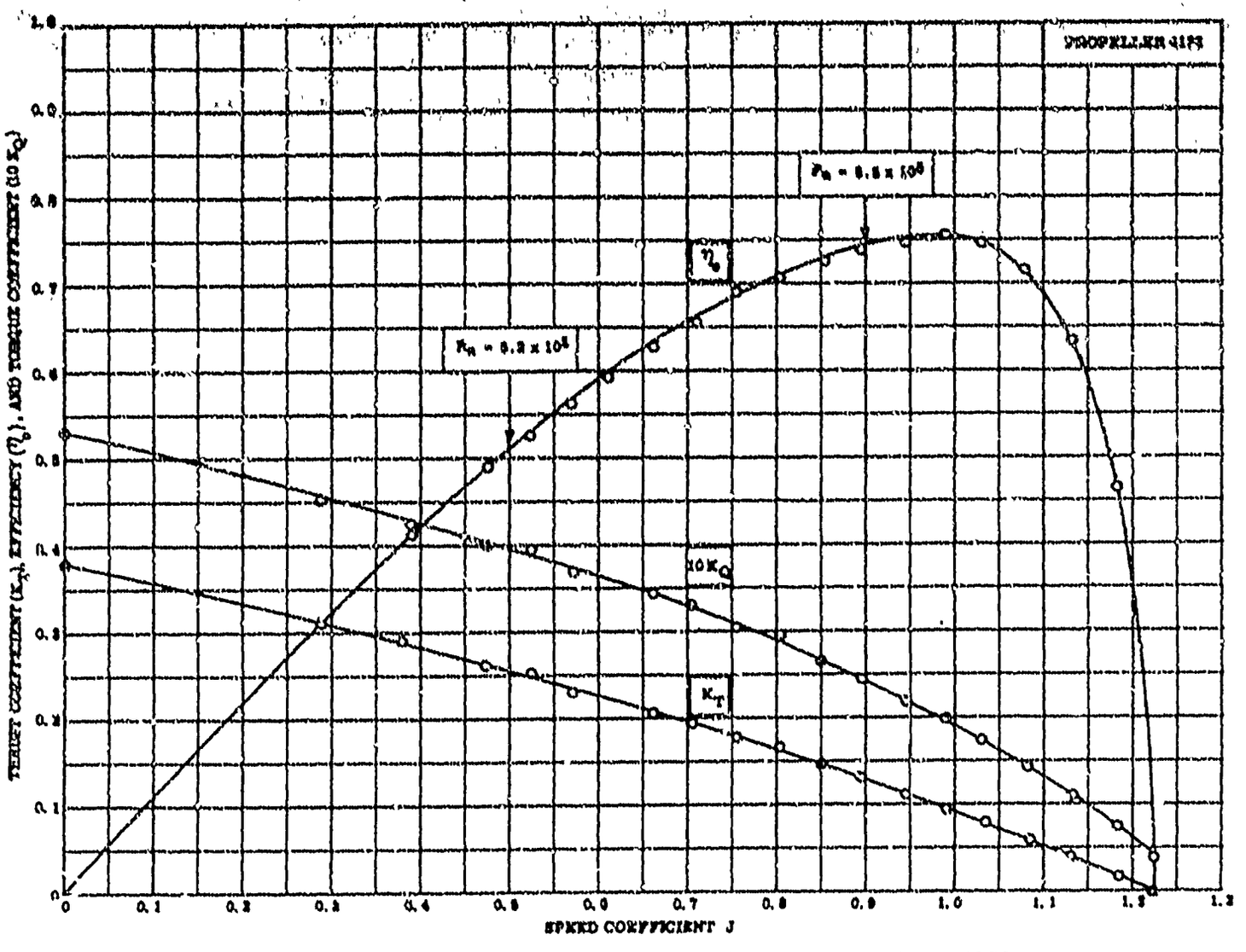

Figure 9 - Open-Water Performance Curves, Propeller 4132

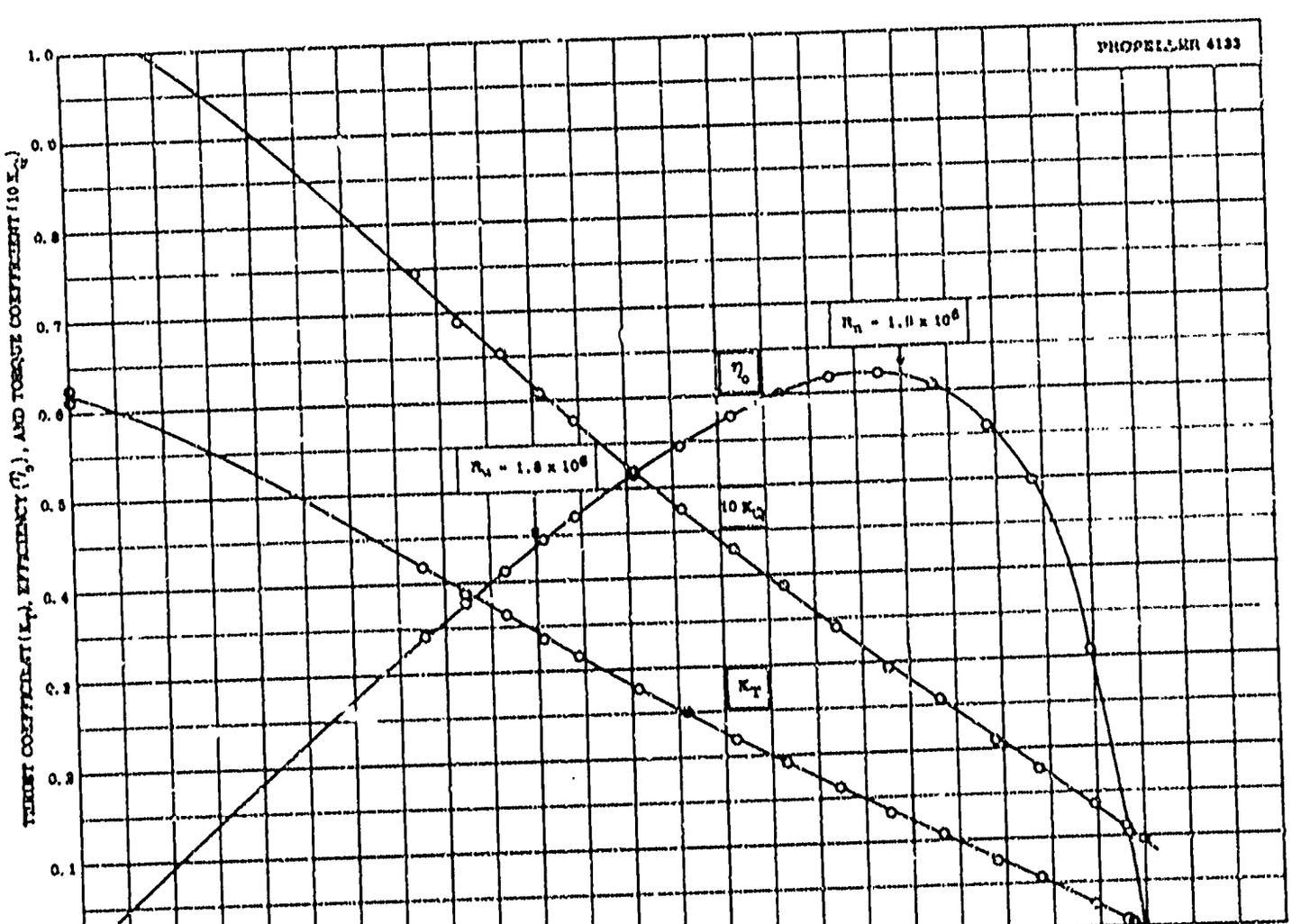

Figure 10 - Open-Water Performance Curves, Propeller 4133

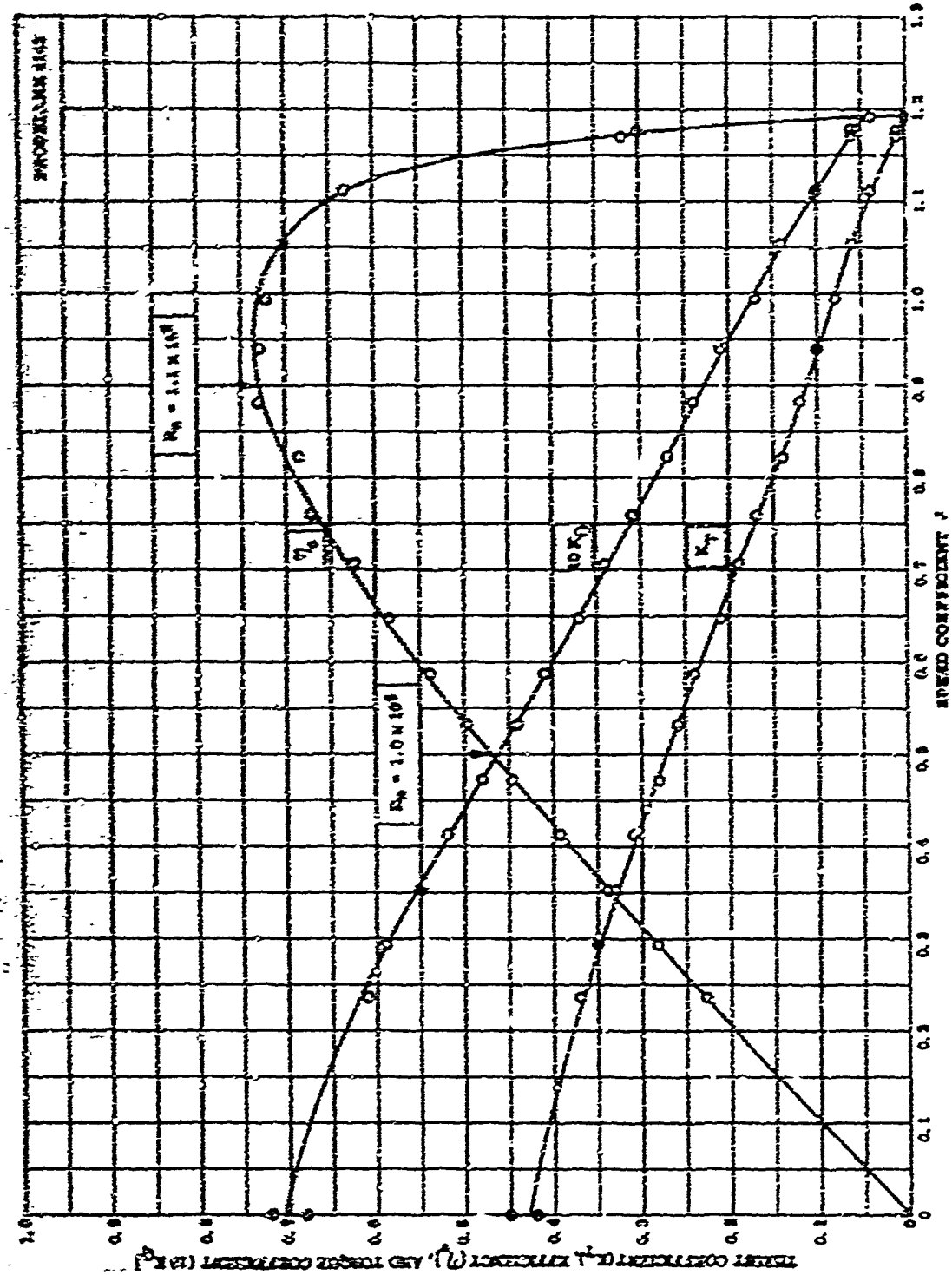

Figure 11 - Open-Water Performance Curves, Propeller 4142

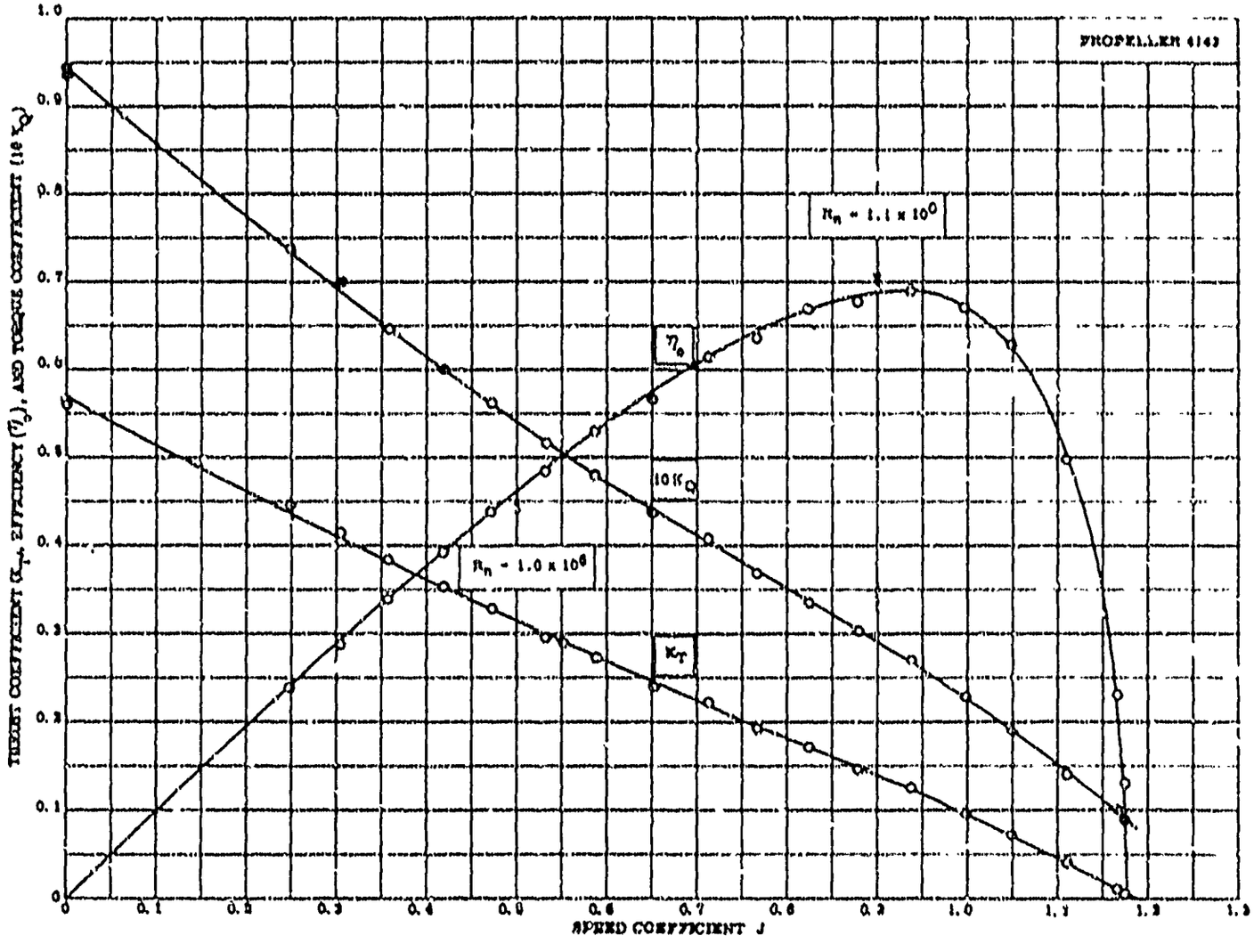

Figure 12 - Open-Water Performance Curves, Propeller 4143

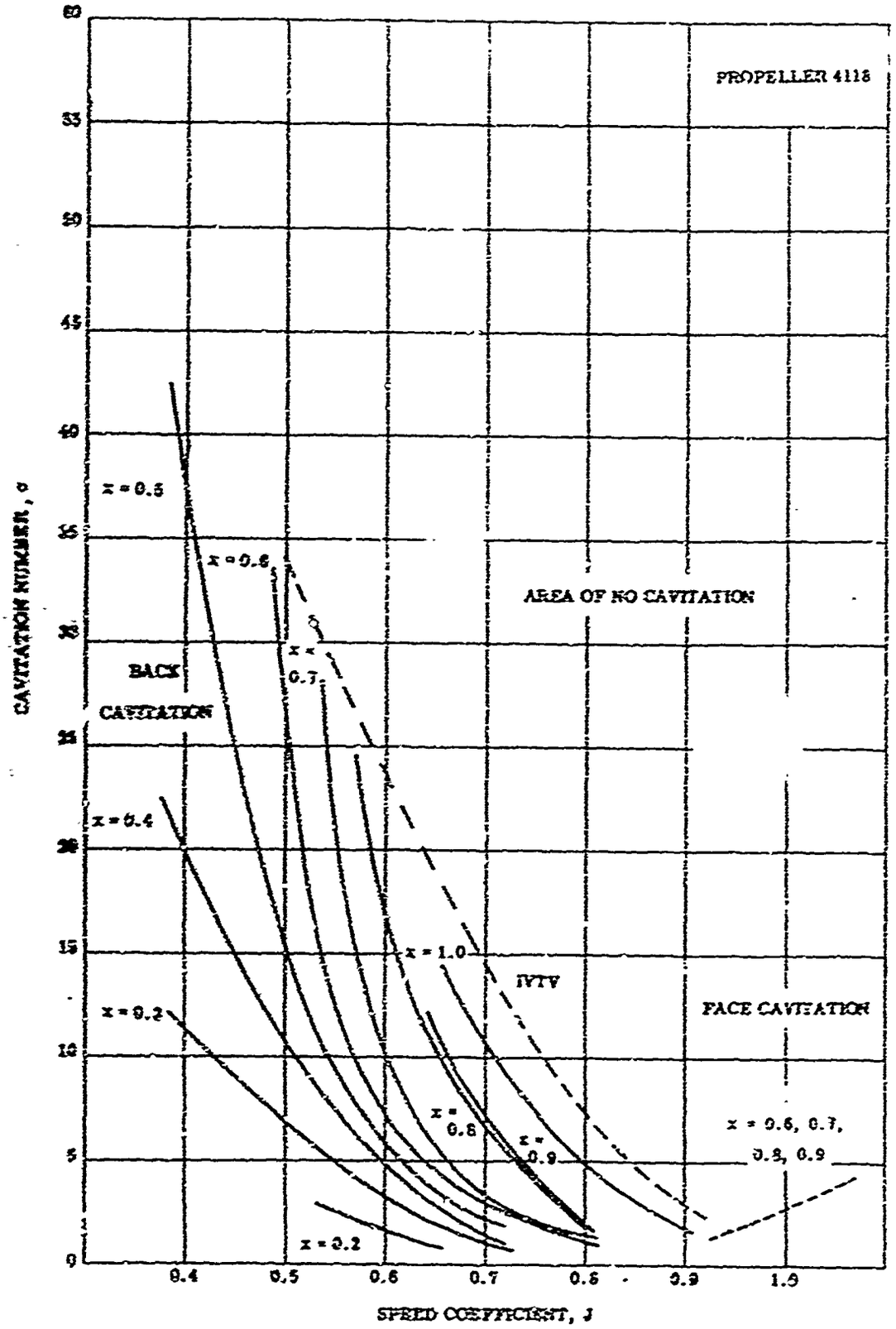

Figure 13 - Cavitation Inception Curves, Propeller 4118

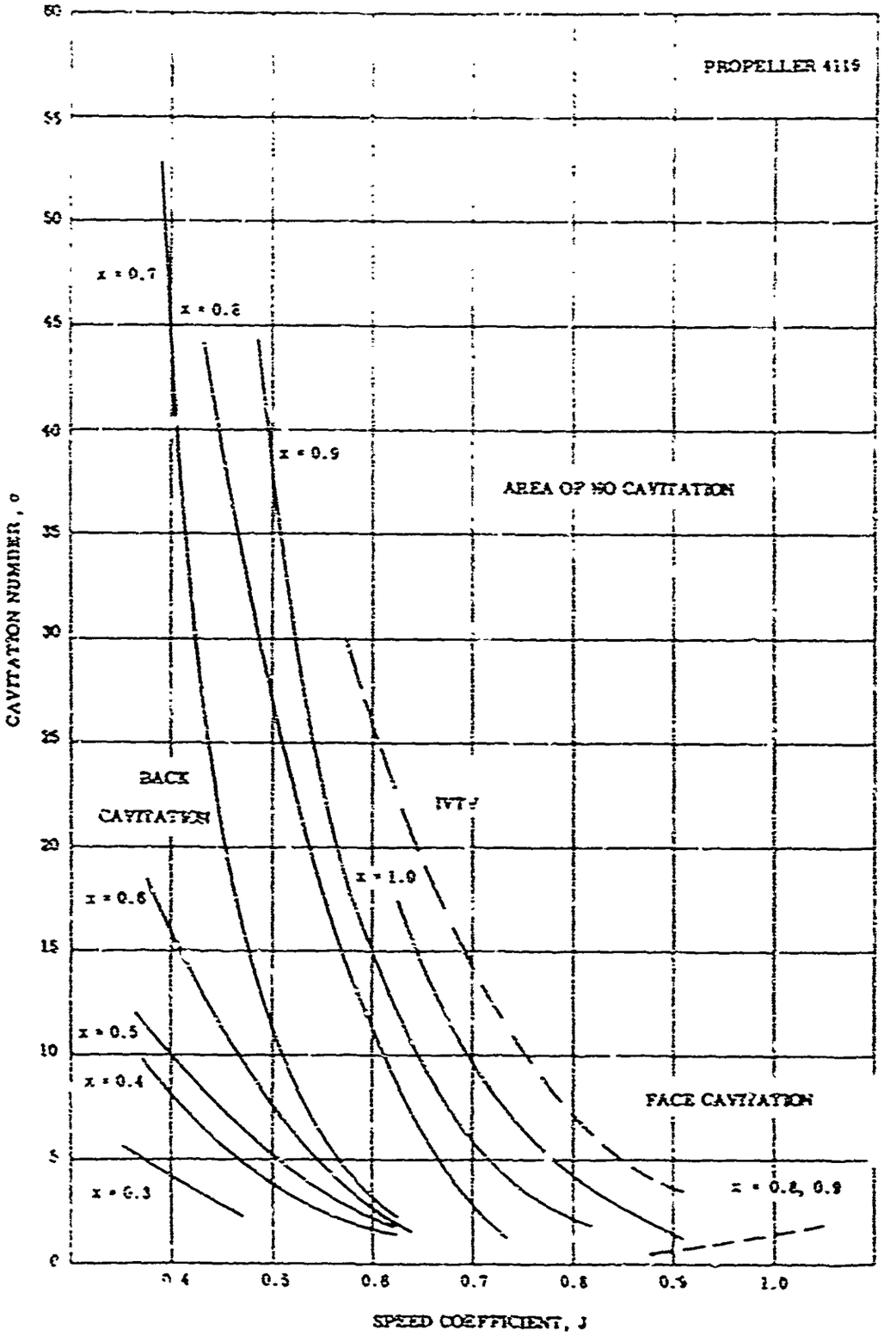

Figure 14 - Cavitation Inception Curves, Propeller 4119

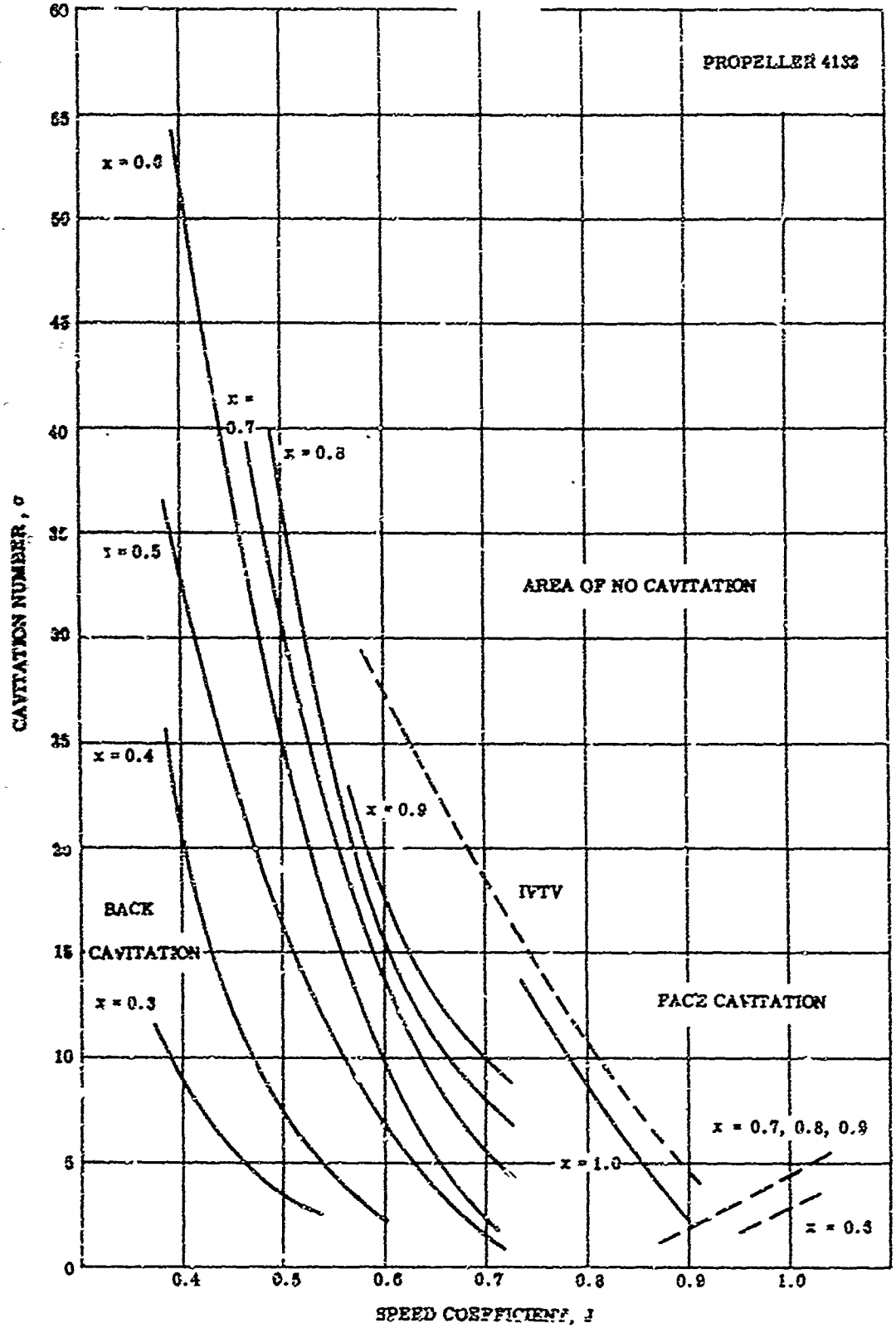

Figure 15 - Cavitation Inception Curves, Propeller 4132

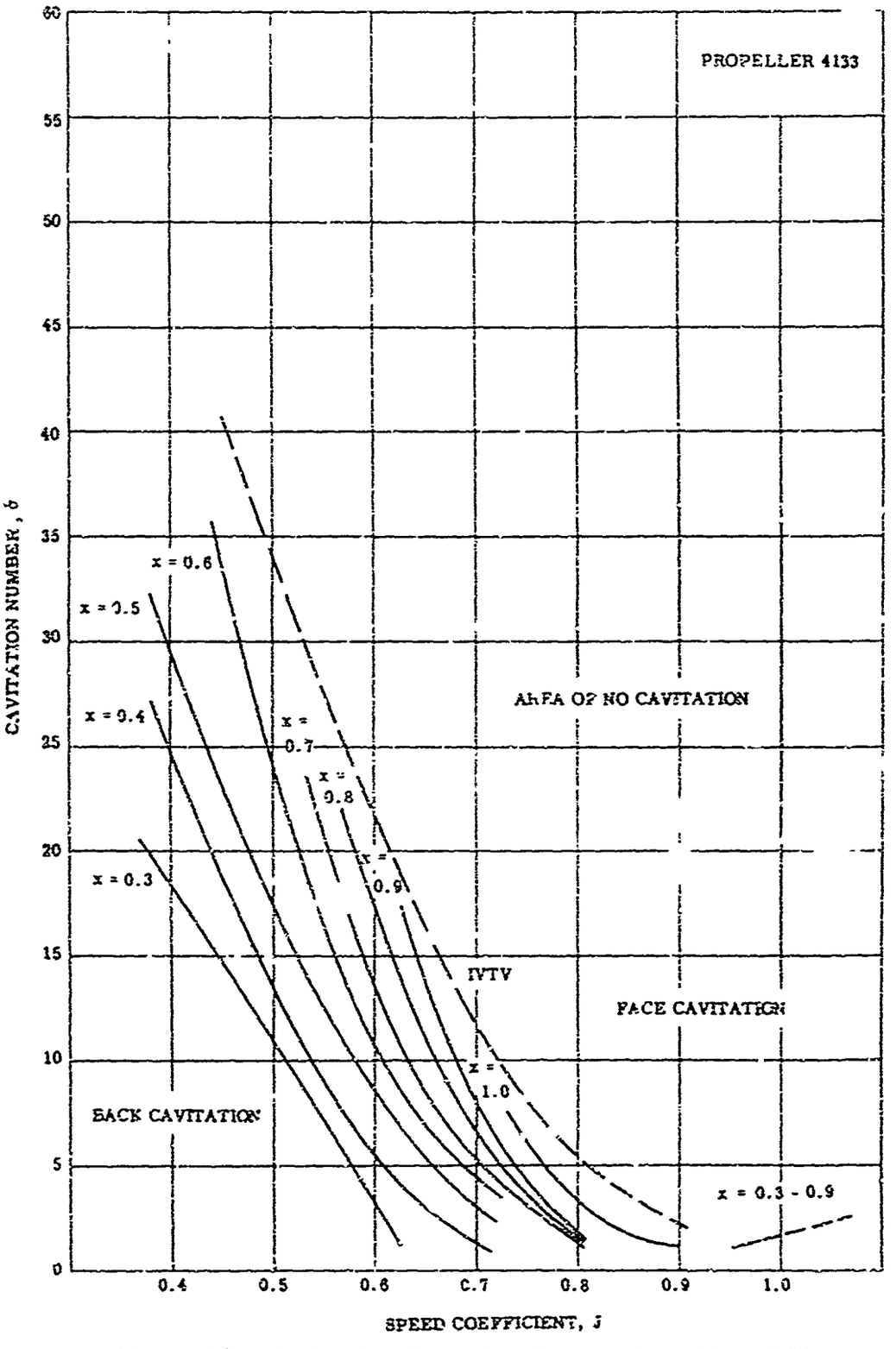

Figure 16 - Cavitation Inception Curves, Propeller 4133

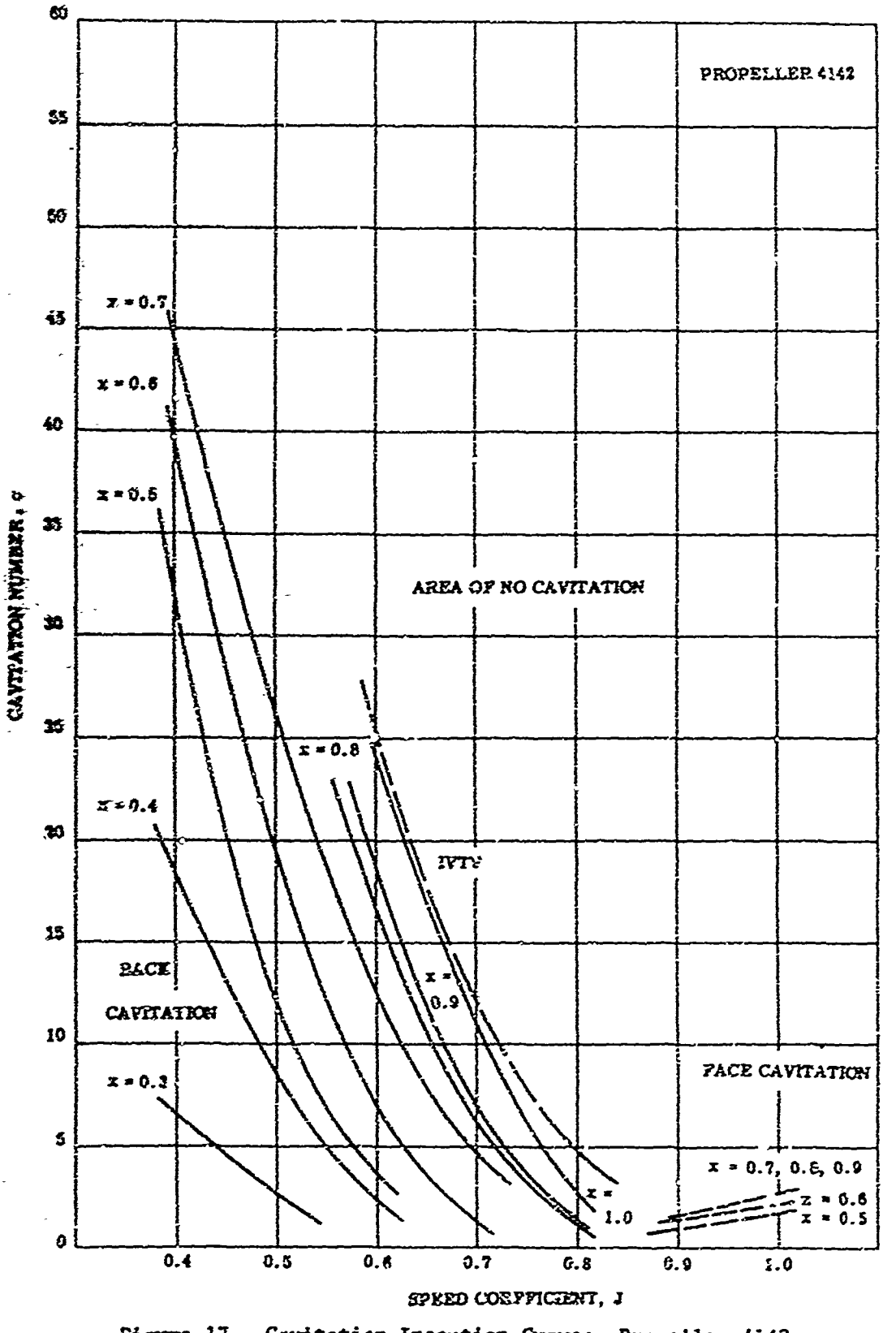

Figure 17 - Cavitation Inception Curves, Propeller 4142

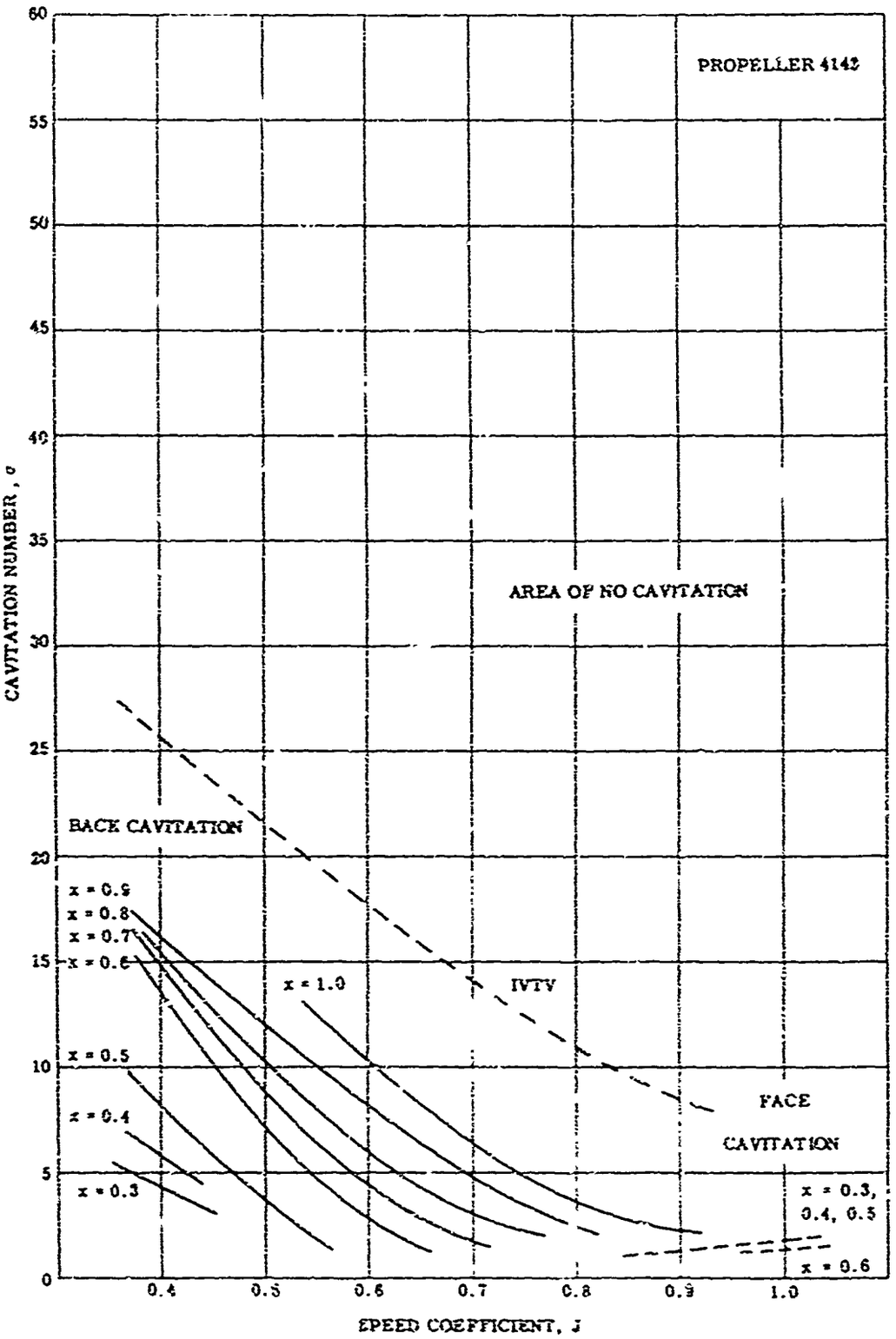

Figure 18 - Cavitation Inception Curves, Propeller 4143

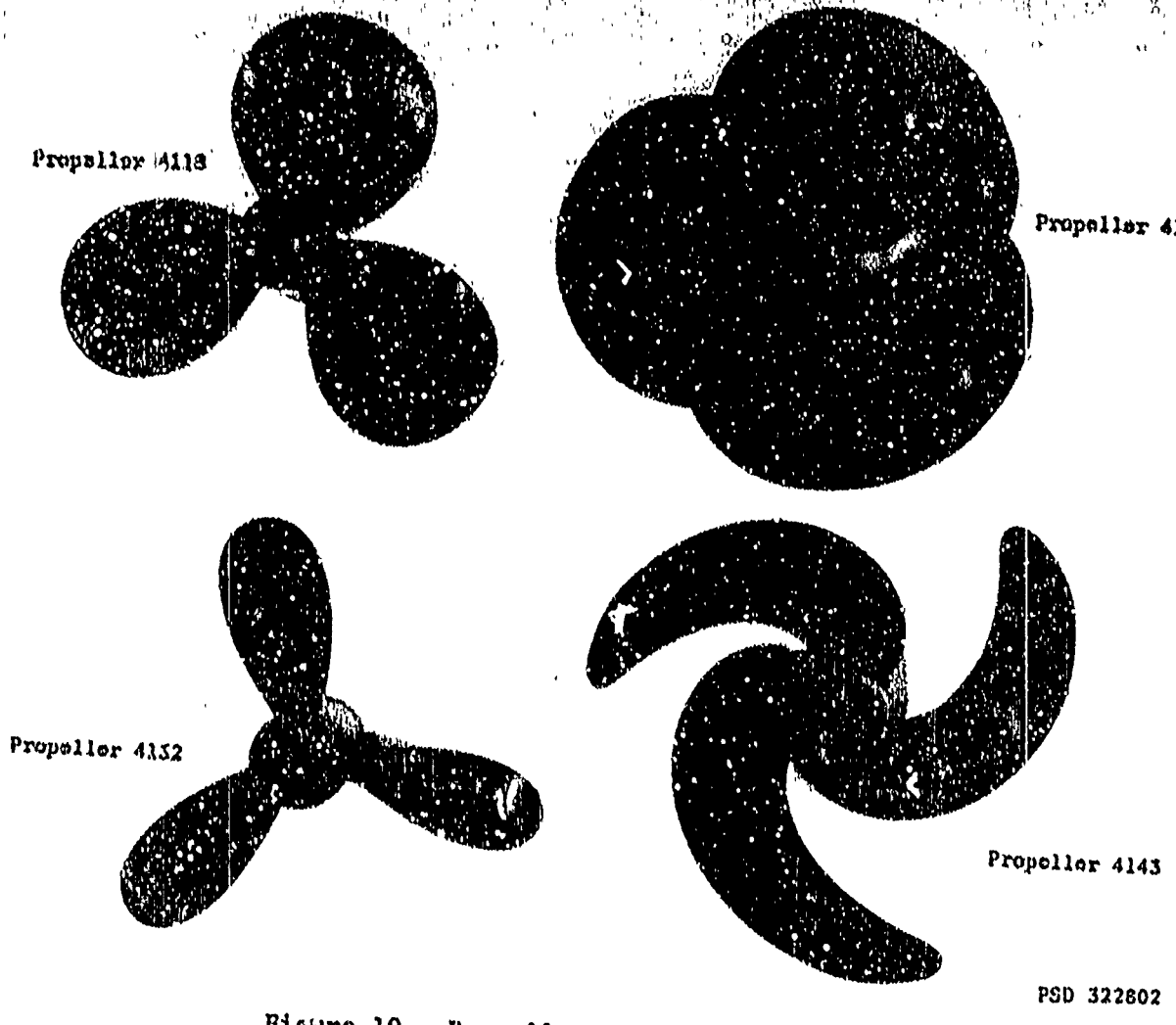

Figure 19 - Propellers 4118, 4132, 4133, 4143

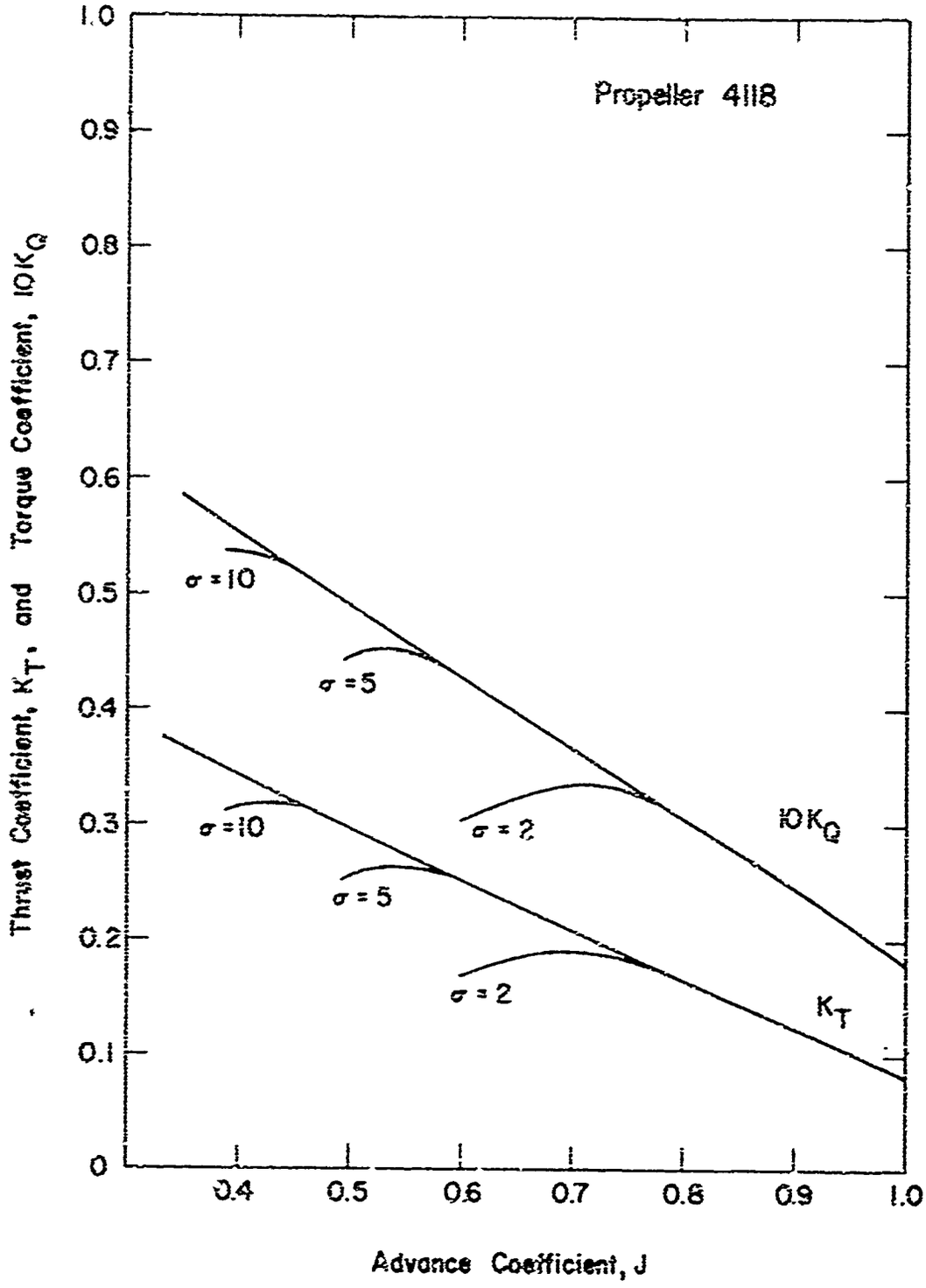

Figure 20 - Cavitation Performance of Propeller 4118 at $\sigma = 2.0$, $\sigma = 5.0$, $c = 10.0$

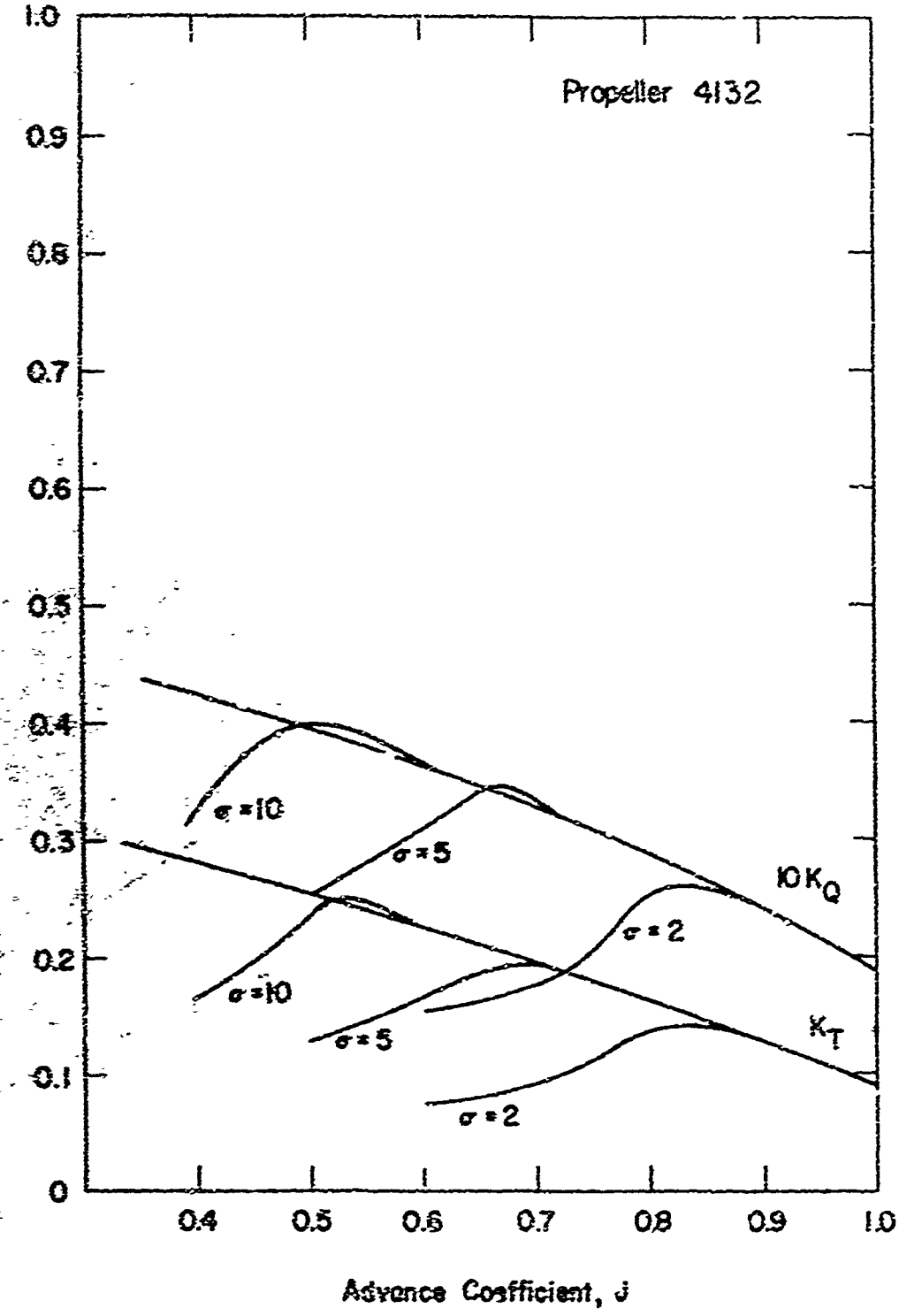

Figure 21 - Cavitation Performance of Propeller 4132 at $\sigma = 2.0$, $\sigma = 5.0$, $\sigma = 10.0$

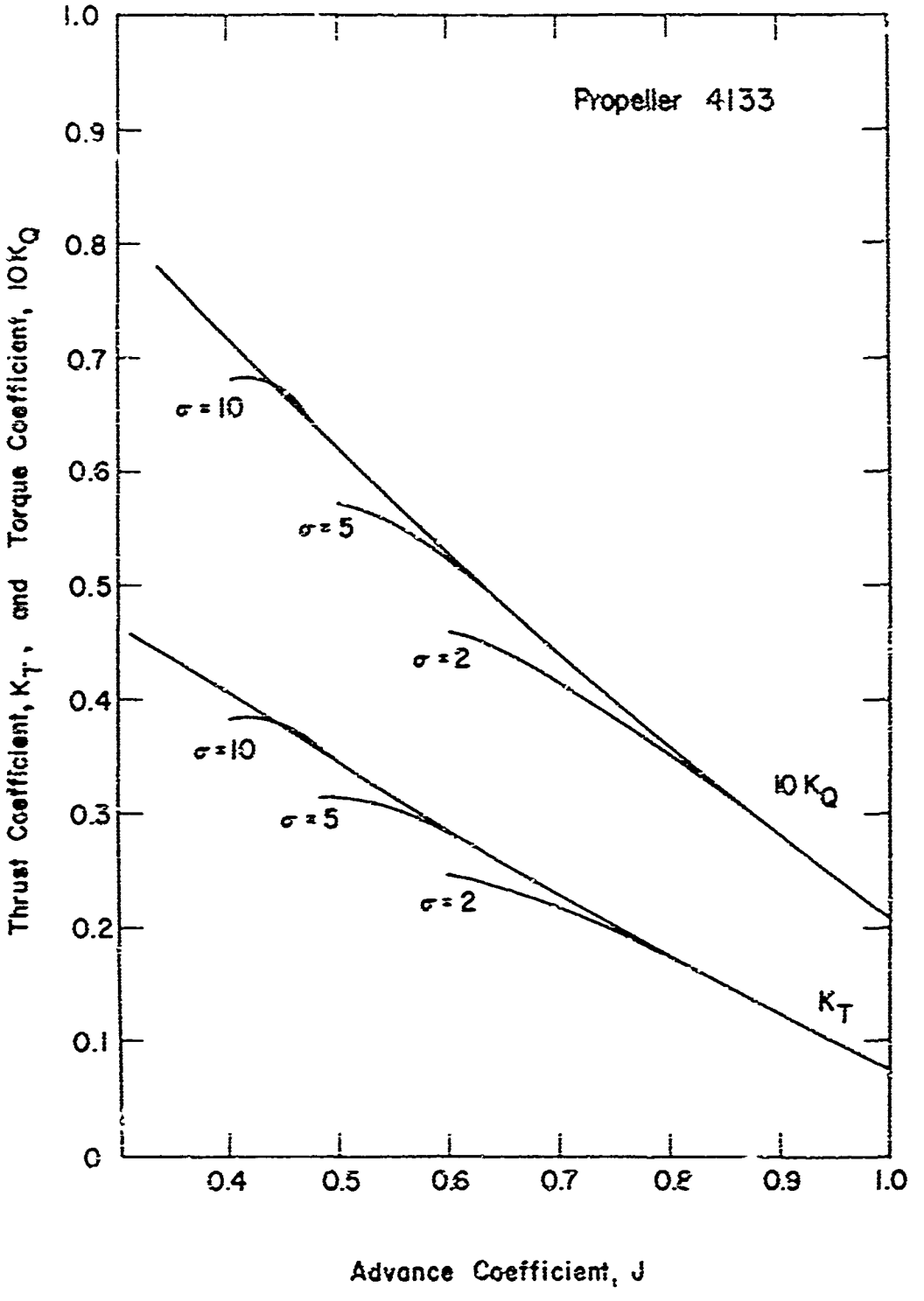

Figure 22 - Cavitation Performance of Propeller 4133 at $\sigma = 2.0$, $\sigma = 5.0$, $\sigma = 10.0$

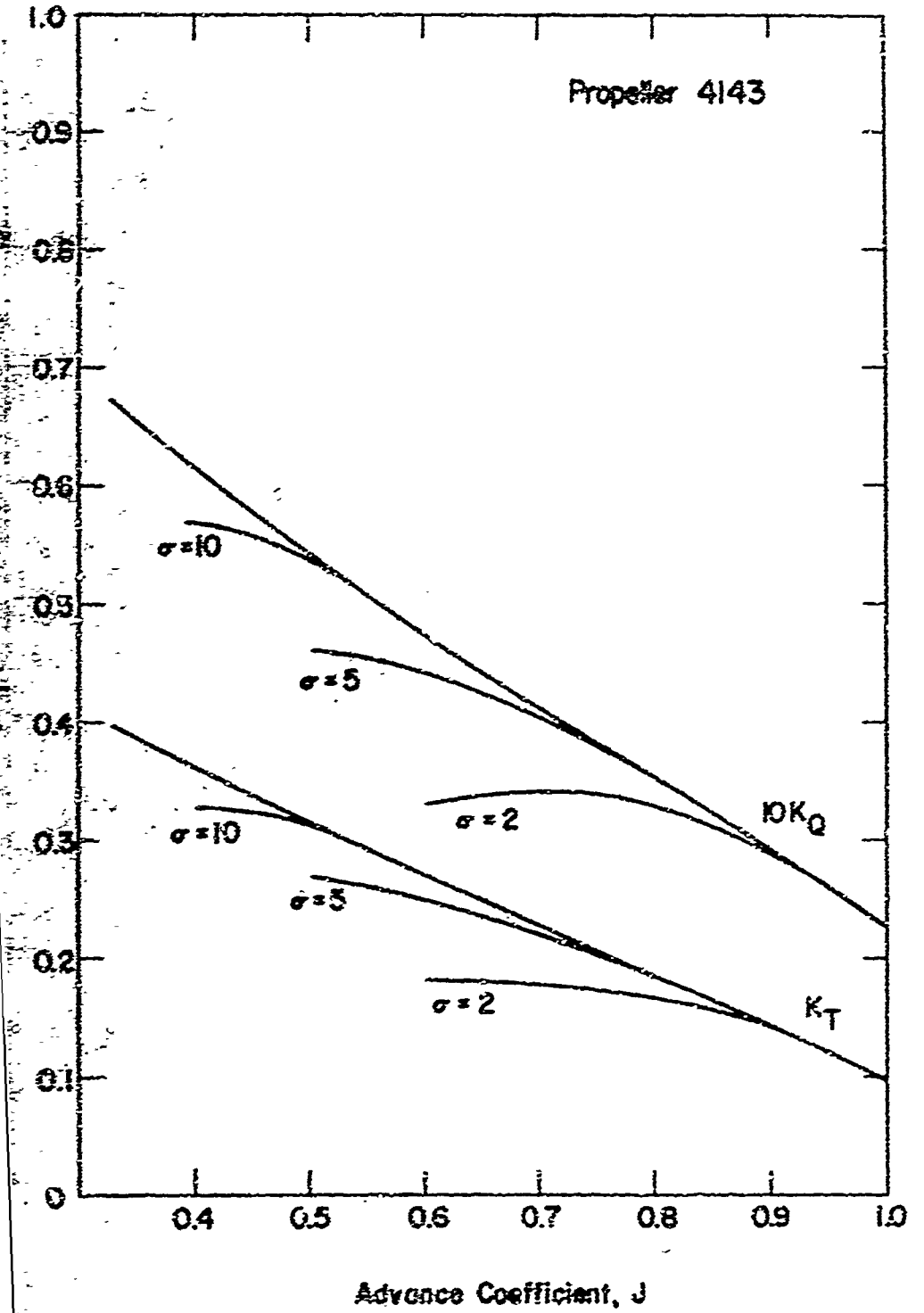

Figure 23 - Cavitation Performance of Propelier 4143 at $\sigma = 2.0$, $\sigma = 5.0$, $\sigma = 10.0$

Propeller 4118

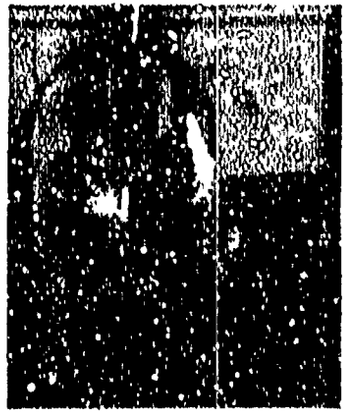

Propeller 4132

Propeller 4133

Propeller 4143

Figure 24 - Propeller Back Cavitation at J = 0.4, σ = 10.0

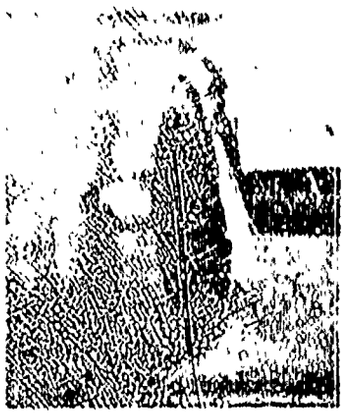

Propeller 4118

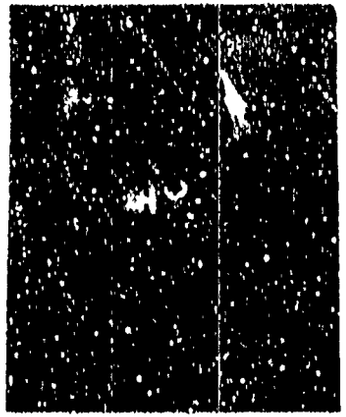

Propeller 4132

Propeller 4133

Propeller 4143

Figure 25 - Propeller Back Cavitation at J = 0.5, σ = 5.0

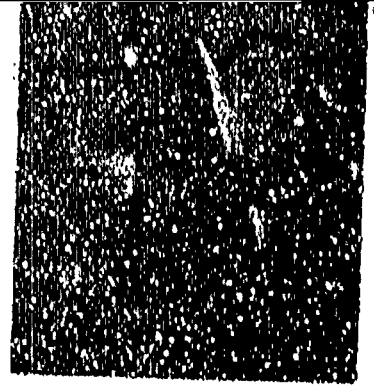

Propeller 4118

Propeller 4132

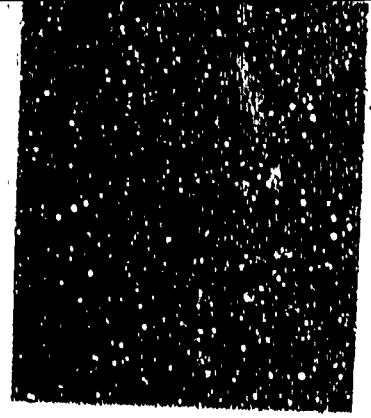

Propeller 4133

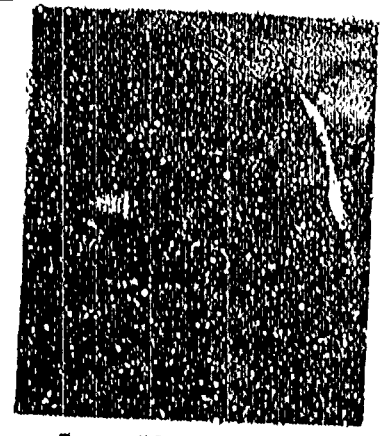

Propeller 4143

Figure 26 - Propeller Back Cavitation at J = 0.6, σ = 5.0

Propeller 4118

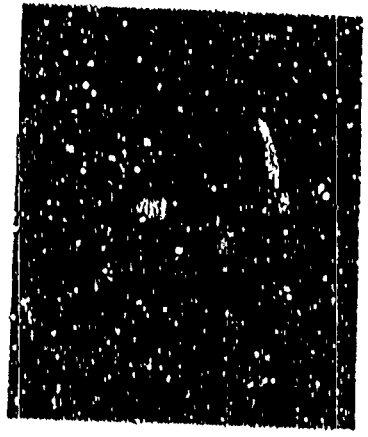

Propeller 4132

Propeller 4133

Propeller 4143

Figure 27 - Propeller Back Cavitation at J = 0.6, σ = 2.0

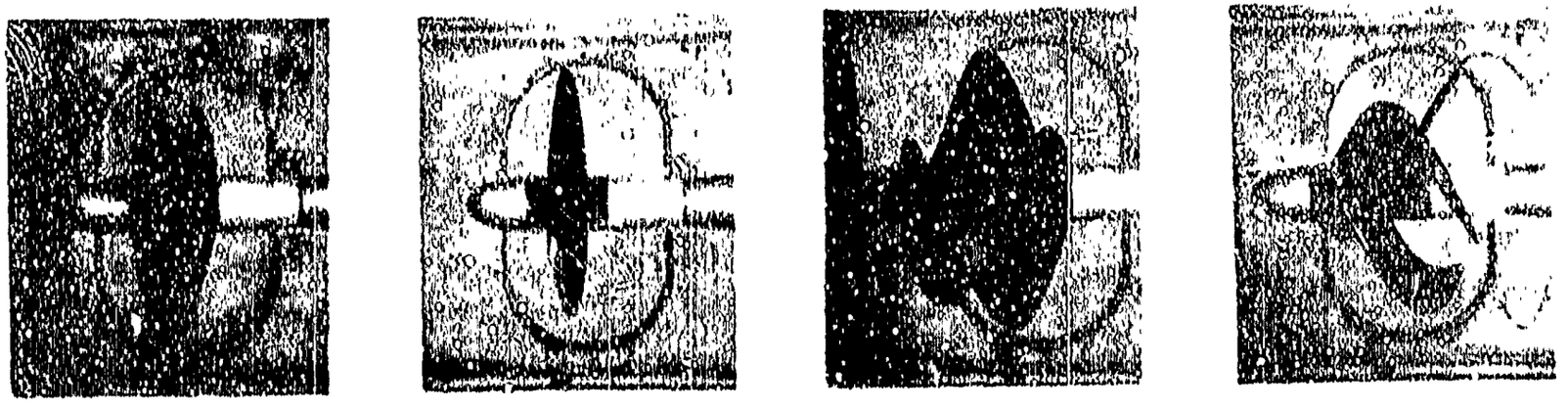

Propeller 4118 | Propeller 41[illegible] | Propeller 4133 | Propeller 4143

Figure 28 - Propeller Face Cavitation at J = 1.0, σ = 2.0

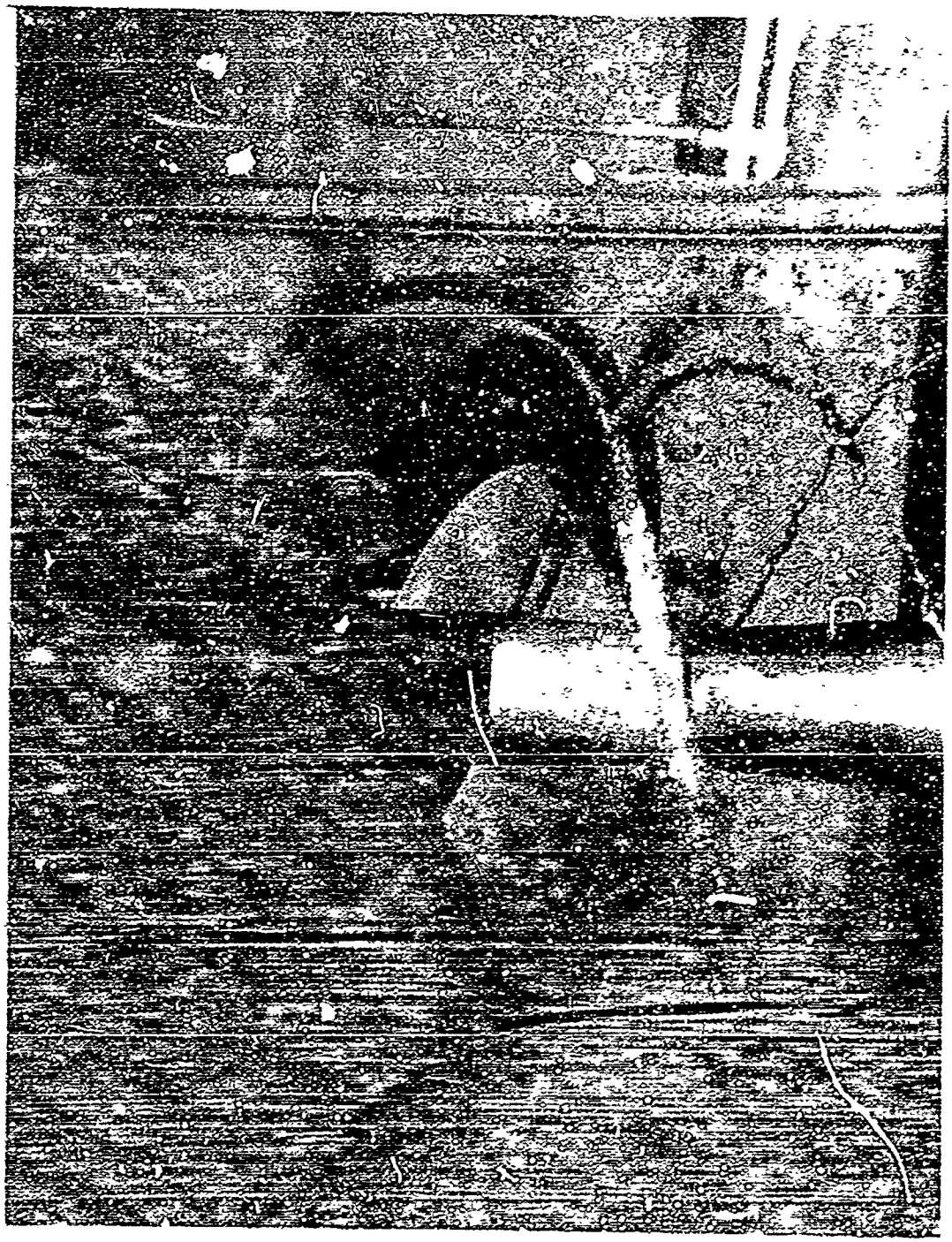

Figure 29 - Back and Trailing Cavitation on Propeller 4143 at $J = 0.8$, $\sigma = 1.7$

TABLE 1

Propeller 4118 Geometry

X	c/D	t/D
0.20	0.3200	0.0439
0.30	0.3635	0.0282
0.40	0.4048	0.0239
0.50	0.4392	0.0198
0.60	0.4610	0.0160
0.70	0.4622	0.0125
0.80	0.4347	0.0091
0.90	0.3613	0.0060
0.95	0.2775	0.0045
1.00	------	------

TABLE 2

Propeller Geometry Variations

Propeller Number	41[illegible]	4119	4132	4133	4142	4143*
No. of Blades	3	3	3	3	3	3
Expanded Area Ratio	0.606	0.606	0.303	1.212	0.606	0.606
Mean Width Ratio	0.397	0.397	0.199	0.794	0.397	0.397
Blade Thickness Fraction	0.040	0.080	0.057	0.028	0.040	0.040
NACA Meanline	0.8	0.8	0.8	0.8	1.0	0.8
P/D at 0.7R	1.077	1.084	1.086	1.073	1.088	1.071
Diameter (inches)	12.0	12.0	12.0	12.0	12.0	12.0

*Propeller 4143 had 15 deg of skew per 0.1 radius for a total skew of tip = 120.0 deg

TABLE 3

P/D Distributions

x	Propeller 4118	Propeller 4119	Propeller 4132	Propeller 4133	Propeller 4142	Propeller 4143
0.2	1.086	1.105	1.090	1.077	1.097	0.925
0.3	1.084	1.102	1.093	1.077	1.095	0.932
0.4	1.082	1.098	1.094	1.076	1.092	0.954
0.5	1.080	1.093	1.091	1.075	1.088	0.991
0.6	1.078	1.088	1.088	1.074	1.088	1.032
0.7	1.077	1.084	1.086	1.073	1.088	1.071
0.8	1.075	1.081	1.085	1.073	1.089	1.120
0.9	1.073	1.078	1.084	1.073	1.090	1.181
1.0	1.070	1.075	1.084	1.073	1.091	1.240

TABLE 4

C_o/c Distributions

x	Propeller 4118	Propeller 4119	Propeller 4132	Propeller 4133	Propeller 4142	Propeller 4143
0.2	0.0224	0.0224	0.0355	0.0190	0.0212	0.0369
0.3	0.0232	0.0232	0.0385	0.0202	0.0204	0.0382
0.4	0.0233	0.0233	0.0390	0.0204	0.0199	0.0388
0.5	0.0218	0.0218	0.0357	0.0190	0.0184	0.0362
0.6	0.0207	0.0207	0.0324	0.0180	0.0178	0.0345
0.7	0.0200	0.0200	0.0301	0.0173	0.0174	0.0331
0.8	0.0197	0.0197	0.0282	0.0166	0.0173	0.0316
0.9	0.0182	0.0182	0.0259	0.0153	0.0167	0.0289
1.0	0.0167	0.0167	0.0235	0.0140	0.0156	0.0256

TABLE 5

α_t, Pitch Correction Due to Thickness

x	Propeller 4118	Propeller 4119	Propeller 4132	Propeller 4133	Propeller 4142	Propeller 4143
0.2	0.476	0.952	0.247	0.349	0.476	0.431
0.3	0.456	0.912	0.306	0.325	0.456	0.356
0.4	0.395	0.790	0.300	0.295	0.395	0.283
0.5	0.306	0.612	0.250	0.261	0.306	0.215
0.6	0.225	0.450	0.196	0.224	0.225	0.157
0.7	0.162	0.324	0.151	0.187	0.162	0.114
0.8	0.115	0.230	0.116	0.148	0.115	0.084
0.9	0.090	0.180	0.098	0.119	0.090	0.062
1.0	0.075	0.150	0.080	0.100	0.075	0.015

TABLE 6

Pitch Error, Propeiler 4143

X	Existing P/D	Correct P/D
0.2	0.925	1.225
0.3	0.932	1.204
0.4	0.954	1.166
0.5	0.991	1.119
0.6	1.032	1.072
0.7	1.071	1.026
0.8	1.121	0.979
0.9	1.181	0.920
1.0	1.240	0.904

TABLE 7

Open-Water Performance at Design Advance Speed

Propeller No.	Coefficients	Design	Open Water	Percent Difference
4118	J	0.833	0.833	0
	K_T	0.154	0.150	-2.7
	$10\ K_Q$	0.290	0.285	-1.7
	η_o	0.706	0.698	-1.1
4119	J	0.833	0.833	0
	K_T	0.154	0.146	-5.2
	$10\ K_Q$	0.290	0.280	-3.4
	η_o	0.706	0.692	-2.0
4122	J	0.833	0.833	0
	K_T	0.156	0.153	-1.9
	$10\ K_Q$	0.276	0.275	-0.4
	η_o	0.752	0.738	-1.9
4133	J	0.833	0.833	0
	K_T	0.150	0.157	+4.7
	$10\ K_Q$	0.319	0.331	+3.8
	η_o	0.625	0.630	+0.8
4148	J	0.833	0.833	0
	K_T	0.154	0.138	-10.4
	$10\ K_Q$	0.290	0.264	-9.0
	η_o	0.706	0.694	-1.7
4143	J	0.833	0.833	0
	K_T	0.154	0.168	+9.1
	$10\ K_Q$	0.290	0.334	+15.2
	η_o	0.706	0.667	-5.5

TABLE 8

Open-Water Performance at Design Thrust

Propeller No.	Coefficients	Design	Open Water	Percent Difference
4118	C_T	0.563	0.563	0
	J	0.833	0.828	-0.6
4119	C_T	0.563	0.563	0
	J	0.833	0.824	-1.0
4132	C_T	0.571	0.571	0
	J	0.833	0.829	-0.5
4133	C_T	0.549	0.549	0
	J	0.833	0.841	+1.0
4142	C_T	0.563	0.563	0
	J	0.833	0.833	-2.6
4143	C_T	0.563	0.563	0
	J	0.833	0.850	+2.0

REFERENCES

1. Kerwin, J.E., "The Solution of Propeller Lifting Surface Problems by Vortex Lattice Methods," Doctoral Thesis submitted to Dept. of Naval Arch. and Marine Eng., MIT (1961).

2. Cheng, H.M., "Hydrodynamic Aspect of Propeller Design Based on Lifting-Surface Theory, Part I, Uniform Chordwise Load Distribution," David Taylor Model Basin Report 1802 (Sep 1964).

3. Cheng, H.M., "Hydrodynamic Aspect of Propeller Design Based on Lifting-Surface Theory, Part II, Arbitrary Chordwise Load Distribution," David Taylor Model Basin Report 1803 (Jun 1965).

4. Cox, G.G., "Correction to the Camber of Constant Pitch Propellers," Quarterly Trans. Royal Institute of Naval Architects (1961).

5. Lerbs, H.W., "Moderately Loading Propellers with a Finite Number of Blades and an Arbitrary Distribution of Circulation," Trans. SNAME, Vol. 60 (1952), pp. 73-117.

6. Kerwin, J.E. and Leopold, R., "Propeller-Incidence Correction Due to Blade Thickness," J. Ship Research, Vol. 7, No. 2 (Oct 1963).

7. Eckhardt, M.K. and Morgan, W.B., "A Propeller Design Method," Trans. SNAME, Vol. 63 (1955), pp. 325-374.

8. Jacobs, E.N. et al., "The Characteristics of 78 Related Airfoil Sections from Tests in the Variable-Density Wind Tunnel," National Advisory Committee for Aeronautics Report 460 (1932).

9. Brockett, T., "Minimum Pressure Envelopes for Modified NACA-66 Sections with NACA a = 0.8 Camber and BuShips Type I and Type II Sections," David Taylor Model Basin Report 1780 (Feb 1966).

10. Kerwin, J.E. and Leopold, R., "A Design Theory for Subcavitating Propellers," Trans. SNAME, Vol. 72 (1964).

11. Thwaites, B. (editor), "Incompressible Aerodynamics," Clarendon Press, Oxford (1960).

12. Pfleiderer, C., "Die Kreiselpumpen fur Flussigkeiten und Gase." Springen-Verlag, Berlin-Gottingen-Heiderberg (1961), pp. 338-340.

13. Jones, R.T., "Effects of Sweepback on Boundary Layer and Separation," National Advisory Committee for Aeronautics Report 884 (1947).

14. Boswell, R.J. and Miller, M.L., "Unsteady Propeller Loading -Measurement, Correlation with Theory, and Parametric Study," Naval Ship Research and Development Report 2625

UNCLASSIFIED

Security Classification

DOCUMENT CONTROL DATA - R & D

(Security classification of title, body of abstract and indexing annotation must be entered when the overall report is classified.)

1. ORIGINATING ACTIVITY (Corporate author)

Naval Ship Research and Development Center
Washington, D.C. 20007

2a. REPORT SECURITY CLASSIFICATION

UNCLASSIFIED

2b. GROUP

3. REPORT TITLE

CAVITATION AND OPEN-WATER PERFORMANCE TESTS OF A SERIES OF PROPELLERS DESIGNED BY LIFTING-SURFACE METHODS

4. DESCRIPTIVE NOTES (Type of report and inclusive dates)

Final Report

5. AUTHOR(S) (First name, middle initial, last name)

Stephen B. Denny

6. REPORT DATE	7a. TOTAL NO. OF PAGES	7b. NO. OF REFS
September 1968	54	14

8a. CONTRACT OR GRANT NO.	9a. ORIGINATOR'S REPORT NUMBER(S)
b. PROJECT NO. Subproject S-R009 01 01	2878
c. Problem Number 526-806	9b. OTHER REPORT NO(S) (Any other numbers that may be assigned this report)
d.	

10. DISTRIBUTION STATEMENT

This document is subject to special export controls and each transmittal to foreign governments or foreign nationals may be made only with prior approval of Naval Ship Research and Development Center, Code 500.

11. SUPPLEMENTARY NOTES	12. SPONSORING MILITARY ACTIVITY

13. ABSTRACT

Results of cavitation inception and performance tests are presented for a series of model propellers designed using lifting-surface procedures. Open-water performance curves are shown in addition to cavitation inception and cavitation performance data obtained in the NSRDC 24-inch variable-pressure water tunnel. The propeller series included geometrical variations of blade area, thickness, skew, and section meanlines. Photographs are presented to compare cavitation on propellers with different blade areas and skew and operating at identical cavitation numbers and advance coefficients.

In open water, the propellers operated near their design performance, indicating that the procedure used for calculating the lifting-surface corrections is satisfactory. For very large blade areas, however, the lifting-surface pitch corrections tended to be high; for extremely thick blade section, the pitch corrections due to thickness were too small to sufficiently account for the altered flow resulting from thick sections. For propellers with constant chordwise loading (a = 1.0 mean line), no suitable modification to two-dimensional sections was found to correct for the increased viscous effects in three-dimensional flow.

DD FORM 1473 (PAGE 1)

S/N 0101-807-6801

UNCLASSIFIED

Security Classification

UNCLASSIFIED

Security Classification

KEY WORDS	LINK A		LINK B		LINK C	
	ROLE	WT	ROLE	WT	ROLE	WT
Marine Propellers						
Cavitation						
Performance						
Lifting Surface Propeller Design						

DD FORM 1 NOV 65 1473 (BACK)

(PAGE 2)

S/N 0101-807-6801

UNCLASSIFIED

Security Classification